JAERI-Data/Code
98-013

EXPERIMENTAL DATA ON POLYETHYLENE SHIELD TRANSMISSION OF QUASI-MONOENERGETIC NEUTRONS GENERATED BY 43-AND 68-MeV PROTONS VIA ^{7}Li(p,n) REACTION

March 1998

Noriaki NAKAO[*1], Hiroshi NAKASHIMA, Makoto NAKAO[*2], Yukio SAKAMOTO, Yoshihiro NAKANE, Susumu TANAKA, Shun-ichi TANAKA and Takashi NAKAMURA[*2]

日本原子力研究所
Japan Atomic Energy Research Institute

本レポートは，日本原子力研究所が不定期に公刊している研究報告書です。
入手の問合わせは，日本原子力研究所研究情報部研究情報課（〒319-1195　茨城県那珂郡東海村）あて，お申し越しください。なお，このほかに財団法人原子力弘済会資料センター（〒319-1195　茨城県那珂郡東海村日本原子力研究所内）で複写による実費頒布をおこなっております。

This report is issued irregularly.
Inquiries about availability of the reports should be addressed to Research Information Division, Department of Intellectual Resources, Japan Atomic Energy Research Institute, Tokai-mura, Naka-gun, Ibaraki-ken, 319-1195, Japan.

編集兼発行　日本原子力研究所
印　　刷　いばらき印刷㈱

JAERI-Data/Code 98-013

Experimental Data on Polyethylene Shield Transmission of Quasi-Monoenergetic Neutrons Generated by 43- and 68-MeV Protons via ^{7}Li(p,n) Reaction

Noriaki NAKAO[*1], Hiroshi NAKASHIMA, Makoto NAKAO[*2],
Yukio SAKAMOTO, Yoshihiro NAKANE, Susumu TANAKA[+2],
Shun-ichi TANAKA[+1] and Takashi NAKAMURA[*2]

Center for Neutron Science
Tokai Research Establishment
Japan Atomic Energy Research Institute
Tokai-mura, Naka-gun, Ibaraki-ken

(Received February 5, 1998)

An experiment on neutron transmission through polyethylene shields up to 183.0 cm in thickness was carried out using the quasi-monoenergetic neutron beam sources by ^{7}Li(p,n) reaction with 43 and 68 MeV protons accelerated by the 90 MV AVF cyclotron at the TIARA facility of JAERI. The energy spectra of the transmitted neutron between 10^{-4} eV and the peak neutron energy were measured by a BC501A scintillation counter and a Bonner ball counter. The counting and reaction rates behind and inside the shields were also measured by the Bonner ball counter, ^{238}U and ^{232}Th fission counters and solid state nuclear track detectors. The neutron dose equivalent behind the shields is also given on the basis of experimental data using a neutron rem counter. All the data in this report are summarized numerically for application to benchmark calculations.

Keywords: Transmission, Polyethylene, Shield, Intermediate Energy, Quasi-Monoenergetic Neutron, Neutron Spectrum, Reaction Rate, Neutron Dose Equivalent, Benchmark Experiment

[+1] Office of Planning

[+2] Advanced Radiation Technology Center, Takasaki Radiation Chemistry Research Establishment

[*1] High Energy Accelerator Research Organization

[*2] Tohoku University

JAERI-Data/Code 98-013

43及び68MeV陽子の^{7}Li(p,n)反応により発生する疑似単色中性子を用いたポリエチレン遮蔽体透過実験における測定データ

日本原子力研究所東海研究所中性子科学研究センター
中尾　徳晶*1・中島　　宏　・中尾　　誠*2・坂本　幸夫
中根　佳弘　・田中　　進+2・田中　俊一+1・中村　尚司*2

(1998年2月5日受理)

原研高崎研の90MV-AVFサイクロトロン施設において、43及び68MeV陽子の^{7}Li(p,n)反応によるビーム状疑似単色中性子源を用いて、183.0cm厚さまでのポリエチレン遮蔽体における中性子透過実験を行った。本実験では、遮蔽体後面においてBC501Aシンチレーション検出器及びボナーボール検出器を用いて中性子エネルギースペクトルを、遮蔽体後面または内部においてボナーボール検出器、^{238}U及び^{232}Th核分裂計数管、固体飛跡検出器を用いて中性子計数率及び反応率を測定した他、遮蔽体後面において中性子レムカウンターによるデータを基に中性子線量当量を求めた。本報告書は、ベンチマーク計算に供するため、これらの実験値を数値データとして纏めたものである。

東海研究所：〒319－1195　茨城県那珂郡東海村白方白根２－４
+1 企画室
+2 高崎研究所放射線高度利用センター
*1 高エネルギー加速器研究機構
*2 東北大学

Contents

目　　次

1. INTRODUCTION

Recently, accelerators are widely used for a variety of purposes such as nuclear physics, medical therapy and industry. In high energy accelerator facilities, the shielding performance for high energy neutrons is of great importance to keep the radiation levels of working area and surrounding environment as low as possible. With the increase of beam current and energy, the facilities require more massive and sophisticated shield structure. The shielding design minimized by high accurate data is inevitable to save the construction cost. The experimental data for shielding are, however, very scarce in the energy range above 20 MeV, because there are few neutron source facilities above 20 MeV which is suitable for shielding experiment and it is difficult to measure neutron spectrum for higher energy. Meulder et al.[1], Shin et al.[2] and Uwamino et al.[3] measured the energy spectra of neutrons transmitted through various shielding materials using broad spectral neutrons up to about 50 MeV. Ishikawa et al.[4] used quasi-monoenergetic neutron sources generated in a thin Li target by 25- and 35-MeV protons for concrete and iron shielding experiments. In the higher energy range, Moritz et al.[5] measured the leakage neutron spectra outside the concrete shielding in the 500-MeV proton accelerator facility.

A polyethylene shielding experiment[6] was performed using the p-^{7}Li quasi-monoenergetic neutrons at the 90-MeV AVF cyclotron facility of the TIARA (Takasaki Ion Accelerator for Advanced Radiation Application) in JAERI (Japan Atomic Energy Research Institute). We have already reported the experimental data of concrete and iron shields.[7,8,9,10] Iron shield is good for high energy neutron attenuation because of large inelastic cross section and high density, but brings out a dominant peak of 10-keV- to 1-MeV-energy in the neutron spectrum behind it. Polyethylene shield is often used behind the iron shield to reduce these low energy neutrons, because of large content of hydrogen which attenuates them most effectively. In this report, we provide the numerical data on polyethylene shielding experiment for 40- and 65-MeV neutrons which are important for shielding design calculation of high energy accelerator facilities. The data compiled here can be used for investigating the accuracy of calculation code and cross section data library.

2. EXPERIMENT

2.1 TIARA facility and experimental set up

The AVF cyclotron facility has been operated since 1992. It has an unique neutron beam course, named as LC-course, arranged for the neutron shielding and cross section experiments. The cross sectional view of the LC-course is shown in Fig. 1. An experiment space of 120 cm x 120 cm x 120 cm is prepared inside the 340-cm-thick concrete shielding wall between the accelerator room and the experimental room. The polyethylene shield of 30.5 to 183.0 cm thickness was assembled on a movable stand with 118.5-cm-wide x 118.0-cm-high x 30.5-cm-thick slabs. The assembly was in contact with the exit of 10.9-cm-diameter collimator located at about 4 m from the ^{7}Li target. Neutron beam is incident to the shield through the collimator when a rotary beam shutter is open, as shown in Fig. 1.

The additional iron collimator shown in Fig. 2 was used for measurements at the position of the off beam axis with thinner shield, 30.5- and 61.0-cm-thick polyethylene, in order to depress the neutron leakage through fillers of iron ball and iron sand, or through rotary shutter of iron and polyethylene which include low density materials or void. Iron collimators of 40 and 80 cm thickness were used for 43- and 68-MeV p-^{7}Li neutron experiments, respectively. Those were assembled with 118.5-cm-wide x 118.0-cm-high iron slabs of 10 cm thickness having a cylindrical hole of 10.9 cm diameter. The densities and the atomic compositions of the polyethylene shield and the additional iron collimator are given in Table 1. The dimensions of shields and collimators for each experiment are summarized in Table 2.

2.2 Neutron sources

The source neutrons were generated by bombarding 43- and 68-MeV protons on 3.6-mm- and 5.2-mm-thick ^{7}Li targets, respectively. The isotopic enrichment of ^{7}Li was 99.9 %. The protons penetrating the target with the 2-MeV energy loss were bent down toward the beam dump by the clearing magnet. Their integrated charge was measured with the current integrator by a Faraday cup for beam current monitoring. The neutrons produced in the forward angle can reach the experimental assembly through the collimator without accompanying protons. The range of the monitored proton currents in this experiment was 0.5 nA to 3 μA.

The absolute flux of source neutrons of the monoenergetic peak per proton beam charge (μC) has been separately obtained from a proton-recoil-counter-telescope (PRT) measurement.[11] The estimated errors of the source neutron peak fluxes by PRT are 3.4 and 3.9 % for 43- and 68-MeV p-Li experiment, respectively. The source neutron fluxes for the shielding experiment were

finally corrected with the neutron attenuation through the rotary shutter exit window of stainless steel, and are given in Table 3.

Two fission chambers of ^{238}U and ^{232}Th placed near the Li target were calibrated to the proton beam current. They were used for monitoring the proton beam current of very low intensity because the current integrator could not work accurately due to the leak current of the Faraday cup. The conversion factors of the monitor counts to total charges of proton beam are also given in Table 3 for the ^{238}U fission chamber.

The spectra of quasi-monoenergetic neutron sources were measured with a BC501A organic liquid scintillation counter using the time of flight (TOF) method. The measured source neutron energy spectra, of which monoenergetic peaks are normalized to unity, are given in Tables 4 and 5. Figure 3 shows the energy spectra multiplied by the absolute peak fluxes of the PRT measurements which are tabulated in Table 3.

2.3 Neutron detectors and data analyses

For the shielding experiment, five kinds of detectors were used for the measurement of neutron spectra and reaction rates behind and inside the polyethylene shields. The detector positions for each experiment are given in Table 2.

2.3.1 BC501A scintillation counter

One of the neutron spectrum measurements in the shielding experiment was performed with the 12.7-cm-diameter x 12.7-cm-long BC501A organic liquid scintillation counter (Bicron Co. Ltd.) coupled to a R4144 photomultiplier (Hamamatsu Photonics. Co. Ltd.). The event-by-event data measured with the BC501A scintillation counter were converted to a two-dimensional distribution of pulse-height and rise-time, and the neutron events were discriminated from the γ-ray events. Then they were converted into the neutron energy spectra using the FERDOU[12] unfolding code and the measured response functions.[13] The responses are exemplified in Fig. 4 and all numerical data are given in Table 6. The energy calibration of the light output pulses was performed at the zero cross point, the Compton edge of 4.43-MeV γ-rays from a ^{241}Am-Be source and the recoiled proton edge of 40- or 65-MeV monoenergetic neutron peak by using the calibration values in Ref.[13]. The difference between the scaler counts of total output pulses and the number of events recorded in the hard disk was used for the dead time correction. Finally the absolute values of the transmitted neutron energy spectra are represented as the flux per proton beam charge (μC) which can be estimated from the fluence monitor counts.

2.3.2 Bonner ball counter

A multi-moderator spectrometer, Bonner ball counter, was also used for measurements of neutron spectra and counting rates behind the polyethylene shields. It has a spherical polyethylene moderator whose thickness is chosen from 0, 1.5, 3.0, 5.0 and 9.0 cm. The thermal neutron detector inserted at the center of the moderator is a 5.08-cm-diameter spherical proportional counter, filled with 10-atm (at 22 °C) ^{3}He gas, made by LND Inc.

The five reaction rates for the five kinds of moderator thickness were unfolded with the SAND-2 code[14] and the response functions given by Uwamino et al.[15] The response functions are shown in Fig. 5 and tabulated in Table 7. Initial guess spectra at each measured position used in the unfolding were obtained from the MORSE[16] calculations with the DLC119/HILO86[17] cross section library. We then obtained the neutron spectra in the energy range from 10^{-4} eV to the peak energy.

2.3.3 Fission counter

The ^{238}U and ^{232}Th fission chambers (Centronic FC480/1000) with 10.1-cm-long x 3.81-cm-diameter active size were used for measuring fission rates behind the polyethylene shield. The absolute efficiencies were calibrated by a ^{252}Cf spontaneous fission neutron source[18] in JAERI. The measured inverse efficiencies are 1.05×10^{3} and 9.86×10^{2} barn/cm^{2}/counts (±4 and 3.4 %), respectively. The fission cross sections of ^{238}U and ^{232}Th have been evaluated up to 20 MeV in JENDL-3[19], and measured by Lisowski et al.[20,21] in the energy region between 20 and 400 MeV. The cross sections are shown in Fig. 6 and the group cross section data are given in Table 8.

2.3.4 Solid state nuclear track detector (SSNTD)

Neutron induced tracks behind and inside the 183.0-cm-thick polyethylene shield were measured using solid state nuclear track detectors which were manufactured by Nagase Landauer Ltd. The composition of the detector is Allyl diglycol carbonate which is the same as that of CR-39. The detector is a rectangular solid of 10 mm x 5 mm and 1-mm-thick on which a 1-mm-thick polyethylene radiator is contacted. After the exposed detectors were etched chemically, the etch pits on the detectors were counted through an optical microscope of 400 times magnifications. The detector response was calculated by a newly-developed Monte Carlo code. The calculated response is shown in Fig. 7 and given in Table 9.

2.3.5 Neutron rem counter

A neutron dose-equivalent detector, neutron rem counter NSN10001 (Fuji Co. Ltd.), was used for measuring neutron dose equivalent rates on the beam axis behind the polyethylene shields. The thermal neutron detector, 5.08-cm-diameter spherical proportional counter filled with ^{3}He gas of 5 atm, are inserted at the center of a 21.0-cm-diameter spherical polyethylene moderator. The moderator is well arranged in terms of its material and geometry so that the response function of the rem counter reproduces the curve of the neutron-flux-to-dose-equivalent conversion factor given by ICRP21[22] as close as possible. The sensitivity of the rem counter is 5 cps for 1 μSv/h, which is calibrated with a ^{252}Cf neutron source.

3. RESULTS

3.1 Neutron spectra measured with the BC501A scintillation counter

The transmitted neutron energy spectra measured with the BC501A scintillation counter are shown in Figs. 8 through 13 and their data are tabulated in Tables 10 through 15. The absolute fluxes are given as lethargy fluxes normalized to a unit proton beam charge (μC) incident to the target. Figures 8 and 11 show the spectra on the beam axis behind the polyethylene shields of 30.5, 61.0, 122.0, and 183.0 cm thickness for 43- and 68-MeV p-Li experiments, respectively. On the other hand, Figs. 9, 10, 12 and 13 show the spectra on the beam axis and at 20- and 40-cm off positions from the beam axis behind 30.5- and 61.0-cm-thick polyethylene shields with the additional iron collimator. The experimental errors of the spectra in the figures include errors of spectrum unfolding and counting statistics in the measurement, conversion factor of fluence monitor counts to total charge of proton beam (3%), neutron penetration factor through objects on the beam line (3%) and the fluence monitor counting statistics (less than 1%).

3.2 Counting rates and neutron spectra measured with the Bonner ball counter

Counting rates behind the polyethylene shields of various thicknesses on the beam axis measured using the Bonner ball counter are shown in Figs. 14 and 15, and their values are given in Tables 16 and 17. Unfolded neutron spectra are shown in Figs. 16 and 17, and the numerical data are given in Tables 18 and 19 for 43- and 68-MeV p-^{7}Li neutron experiments, respectively. The experimental errors of the neutron spectra unfolded with the SAND-2 unfolding code are considered to be 50 to 200 % which are caused by initial guess spectra and iteration processes depending on the analyses.

3.3 Fission rates measured with fission counters

Fission rates measured behind the polyethylene shields of various thicknesses using ^{238}U and ^{232}Th fission counters are shown in Fig. 18, and given in Table 20. The fission rates correspond to the integrated neutron flux in the energy region above ~1 MeV where their fission cross sections are dominant. The errors include the statistical error of each detector counting and other errors described in section 3.1.

3.4 Track rates measured with SSNTD

The track rates of SSNTD measured behind and inside the 183.0-cm-thick polyethylene shield are shown in Fig. 19 and given in Table 21. As shown in Fig. 7, the efficiency of the detector is dominated by the neutrons in the energy region lower than about 10 MeV. The errors include the statistical error of each detector counting and other errors described in section 3.1.

3.5 Neutron dose equivalent

The neutron dose equivalents measured with the neutron rem counter are tabulated in Table 22. Neutron dose equivalents were also estimated from the measured neutron spectra and the ICRP21 neutron flux-to-dose-equivalent conversion factor[22], and are given in Table 23. These measured neutron spectra were obtained from the results above 10 MeV of the BC501A scintillation counter and those below 10 MeV of the Bonner ball counter. The contributions to the dose equivalent of the neutrons above 10 MeV were 88-94 % and 94-97% for 43- and 68-MeV p-Li experiments, respectively. The dose equivalents at 0 cm thickness are estimated using source neutron spectra (see Tables 4 and 5), and peak fluxes (see Table 3).

The neutron dose equivalents are compared in Fig. 20. As seen in the figure, the neutron dose equivalents by the neutron rem counter are underestimated at all the thicknesses compared to those estimated from the measured neutron energy spectra. And their discrepancies were almost constant at all thicknesses because the neutrons spectra behind the various thicknesses of polyethylene shield were relatively similar as seen in Figs. 16 and 17. On the other hand, behind the thicker iron shields (see Figs. 18 and 19 in Ref.[10]), the low energy neutrons are dominant in the spectra, and the neutron dose equivalents by the rem counter and those estimated from the energy spectra comparably agreed (see Fig. 23 in Ref.[10]). This fact reflects that the response function of the rem counter above 20 MeV energy region is lower than the curve of the neutron flux-to-dose-equivalent conversion factor.

4. SUMMARY

Neutrons behind and inside the polyethylene shields of thickness up to 183.0 cm were measured using the 43- and 68-MeV p-^{7}Li neutron sources in the TIARA facility. Neutron spectra in the energy range between 10^{-4} eV and the energies of peak neutrons by the BC501A scintillation counter and the Bonner ball counter, and counting rates by the Bonner ball counter, ^{238}U and ^{232}Th fission counters and SSNTD were obtained. Neutron dose equivalents were also measured by the neutron rem counter, and they give underestimation comparing with those estimated from the measured neutron energy spectra because of the problem for the response function of the rem counter above 20 MeV energy range.

These measured absolute values of neutron energy spectra and reaction rates behind the polyethylene shields are useful to estimate the accuracy of the calculation codes and cross section data sets in the several tens MeV energy range as an integral benchmark data.

ACKNOWLEDGMENT

We wish to thank the operation staff of the TIARA facility for their helpful cooperation during the experiment. This work was conducted as a Universities-JAERI Collaborative Project Research Program.

REFERENCES

1. Meulders J. P., Leleux P., Macq P. C., Pirart C. and Valenduc G., " Intensity Measurements and Shielding of a Fast-neutron Beam for Biological and Medical Applications," Nucl. Instrum. Methods., 126, 81 (1975).
2. Shin K., Ishii Y., Uwamino Y., Sakai H. and Numata S., "Transmission of medium energy neutrons through concrete shields," Radi. Pro. Dosi., 37, No.3, 175 (1991).
3. Uwamino Y., Nakamura T. and Shin K., " Penetration Through Shielding Materials of Secondary Neutrons and Photons Generated by 52-MeV Protons," Nucl. Sci. Eng., 80, 360 (1982).
4. Ishikawa T., Miyama Y. and Nakamura T., "Neutron Penetration Through Iron and Concrete Shields with the Use of 22.0- and 32.5-MeV Quasi-Monoenergetic Sources," Nucl. Sci. Eng., 116, 278 (1994).
5. Moritz L. E., "Measurement of Neutron Leakage Spectra at a 500-MeV Proton Accelerator," Health Phys, 56, No.3, 278 (1989).
6. Nakao N., Nakao M., Nakashima H., Tanaka Su., Sakamoto Y., Nakane Y., Tanaka Sh., and Nakamura T., "Measurements and Calculations of Neutron Energy Spectra Behind Polyethylene Shields Bombarded by 40- and 65-MeV Quasi-Monoenergetic Neutron Sources," J. Nucl. Sci. Technol., Vol.34, No.4, p348 (1997).
7. Nakao N., Nakashima H., Nakamura T., Tanaka Sh., Tanaka Su., Shin K., Baba M., Sakamoto Y. and Nakane Y., "Transmission through shields of quasi-monoenergetic neutrons generated by 43- and 68-MeV Protons : Part I - Concrete Shielding Experiment and Calculation for Practical Application," Nucl. Sci. Eng., 124,228 (1996).
8. Nakashima H., Nakao N., Tanaka Sh., Nakamura T., Shin K., Tanaka Su., Takada H., Meigo S., Sakamoto Y., Nakane Y. and Baba M., "Transmission through shields of quasi-monoenergetic neutrons generated by 43- and 68-MeV Protons : Part II - Iron Shielding Experiment and Analysis for Investigating Calculation Methods and Cross Section Data," Nucl. Sci. Eng., 124,243 (1996).
9. Nakao N., Nakashima H., Sakamoto Y., Nakane Y., Tanaka Sh., Tanaka Su., Nakamura T., Shin K., and Baba M., "Experimental Data on Concrete Shield Transmission of Quasi-monoenergetic Neutrons Generated by 43- and 68-MeV Protons via the ^{7}Li(p,n) reaction", JAERI-Data/Code 97-020 (1997).
10. Nakashima H., Nakao N., Tanaka Sh., Nakamura T., Shin K., Tanaka Su., Meigo S., Nakane Y., Takada H., Sakamoto Y. and Baba M., "Experiments on Iron Shield Transmission of Quasi-monoenergetic Neutrons Generated by 43- and 68-MeV Protons via the ^{7}Li(p,n) reaction", JAERI-Data/Code 96-005 (1996).

11. Baba M., Iwasaki T., Kiyosumi T., Yoshioka Y., Matsuyama S., Hirakawa N., Nakamura T., Tanaka Su., Tanaka Sh., Nakashima H., Meigo S. and Tanaka R., "Characterization and Application of 20-90 MeV ^{7}Li(p,n) Neutron Source at TIARA," Proceedings of International Conference on Nuclear Data for Science and Technology, Gatlinburg Tennessee, U.S.A., Vol.1, 90, (1994).
12. Shin K., Uwamino Y. and Hyodo T., "Propagation of errors from response functions to unfolded spectrum," Nucl. Technol., 53,78 (1981).
13. Nakao N., Nakamura T., Baba B., Uwamino Y., Nakanishi N., Nakashima H. and Tanaka Sh., "Measurements of response function of organic liquid scintillator for neutron energy range up to 135MeV," Nucl. Instrum. Methods., A362, 454 (1995).
14. McElroy W. N., Berg S., Crockett T. and Hawkins R. G., "A computer automated iterative method for neutron flux spectra determination by foil activation," AFWL-TR-67-41, Air Force Weapons Laboratory, Kirtland Air Force Base, vol. 1-4 (1967).
15. Uwamino Y., Nakamura T. and Hara A., "Two types of multi-moderator neutron spectrometers : gamma-ray insensitive type and high-efficiency type," Nucl. Instrum. Methods., A239, 299 (1985).
16. Straker G. R., Steven P. N., Irving D. C. and Cain V. R., "MORSE Code - A Multigroup Neutron and Gamma Ray Monte Carlo Transport Code," ORNL-4585, Oak Ridge National Laboratory, (1970).
17. Alsmiller Jr. R. G., Barnes J. M. and Drischler J. D., "Neutron-Photon Multigroup Cross Sections for Neutron Energies up to 400 MeV (Revision 1)," ORNL/TM-9801, Oak Ridge National Laboratory (1986).
18. Yoshizawa M., Private communication.
19. Shibata K. et al., "Japanese Evaluated Nuclear Data Library, Version-3 -JENDL-3-," JAERI 1319, Japan Atomic Energy Research Institute (1990).
20. Lisowski P. W. et al., "Neutron Induced Fission Cross Section Rates for ^{232}Th, ^{235,238}U, ^{237}Np and ^{239}Pu from 1 to 400 MeV," Proc. Int. Conf. Nuclear Data for Sci. and Technol., Mito, Japan, p.97-99 (1988).
21. Lisowski P. W. et al., "Fission Cross Sections in the Intermediate Energy Region," Proc. Spec. Meet. on Neutron Cross Section Standards for the Energy Region above 20 MeV, Uppsala, Sweden, 21-23 May, 1991, p.177-186 (1991).
22. "Data for Use in Protection Against External Radiation," Ann. ICRP, 17, 2/3 (1987).

Table 1 Density and atomic compositions of the polyethylene shield and the iron collimator.

Material	Density [g cm^{-3}]	Atom	Atomic Density [x10^{22} cm^{-3}]
Polyethylene	0.96	Hydrogen	4.124
		Carbon	8.305
Iron	7.87	Iron	8.487

Table 2 Dimensions of the polyethylene shield and additional collimator, and detector positions.

Ep [a] [MeV]	Shield thickness [cm]	Collimator thickness [cm]	Distance from target to shield [cm]	Detector position (distance from beam axis) [cm]				
				BC501A [b]	Bonner [c]	F.C. [d]	SSNTD [e]	Rem [f]
43	30.5	0	403	0	0	0	0	0
	61.0	0	403	0	0	0	0	0
	122.0	0	403	0	0	0	0	0
	183.0	0	403	0	0	0	0	0
	30.5	40	443	0, 20, 40	-	-	-	-
	61.0	40	443	0, 20, 40	-	-	-	-
68	30.5	0	403	0	0	0	0	0
	61.0	0	403	0	0	0	0	0
	122.0	0	403	0	0	0	0	0
	183.0	0	403	0	0	0	0	0
	30.5	80	483	0, 20, 40	-	-	-	-
	61.0	80	483	0, 20, 40	-	-	-	-

SSNTD detectors were placed behind and inside the 183.0-cm-thick polyethylene shield. The other detectors were placed behind the polyethylene shields of each thickness.

a Proton energy

b BC501A scintillation counter

c Bonner ball counter

d ^{238}U and ^{232}Th fission counters

e Solid state nuclear track detector

f Rem counter

Table 3 Peak fluxes of source neutrons measured with PRT detector and calibrated count rates of ^{238}U fission chamber fluence monitor.

Ep	Peak flux			FC count rate	
[MeV]	[n sr^{-1} μC^{-1}]	(Error)	[n cm^{-2} μC^{-1}]*	[counts μC^{-1}]	(Error)
43	3.45×10^{9}	(±4%)	2.12×10^{4}	1.70×10^{3}	(±3%)
68	4.17×10^{9}	(±5%)	2.94×10^{4}	2.90×10^{3}	(±3%)

* Neutron flux at 403 cm from the target

Table 4 Energy spectrum of 43-MeV p-^{7}Li source neutrons.

Energy Boundary [MeV]	Flux	Error	Energy Boundary [MeV]	Flux	Error
- 6.5[a]	4.405E-02[b]		25.5 - 26.5	4.097E-02	1.77E-03
			26.5 - 27.5	3.960E-02	1.70E-03
6.5 - 7.5	4.405E-02	1.51E-03	27.5 - 28.5	3.473E-02	1.50E-03
7.5 - 8.5	4.423E-02	1.52E-03	28.5 - 29.5	3.491E-02	1.51E-03
8.5 - 9.5	4.483E-02	1.54E-03	29.5 - 30.5	3.081E-02	1.34E-03
9.5 - 10.5	4.503E-02	1.54E-03	30.5 - 31.5	2.639E-02	1.16E-03
10.5 - 11.5	4.390E-02	1.51E-03	31.5 - 32.5	2.097E-02	9.43E-04
11.5 - 12.5	4.501E-02	1.51E-03	32.5 - 33.5	1.875E-02	1.19E-03
12.5 - 13.5	4.633E-02	1.57E-03	33.5 - 34.5	1.490E-02	9.60E-04
13.5 - 14.5	4.931E-02	1.65E-03	34.5 - 35.5	1.290E-02	8.40E-04
14.5 - 15.5	4.895E-02	1.65E-03	35.5 - 36.5	1.083E-02	7.11E-04
15.5 - 16.5	4.885E-02	1.62E-03	36.5 - 37.5	7.232E-03	4.91E-04
16.5 - 17.5	4.752E-02	1.57E-03	37.5 - 38.5	1.337E-02	8.53E-04
17.5 - 18.5	4.977E-02	1.63E-03	38.5 - 39.5	1.377E-01	8.31E-03
18.5 - 19.5	4.611E-02	1.51E-03	39.5 - 40.5	3.629E-01	2.18E-02
19.5 - 20.5	4.707E-02	1.56E-03	40.5 - 41.5	3.677E-01	2.21E-02
20.5 - 21.5	4.749E-02	2.05E-03	41.5 - 42.5	1.135E-01	6.86E-03
21.5 - 22.5	4.686E-02	2.02E-03	42.5 - 43.5	5.063E-03	3.54E-04
22.5 - 23.5	4.653E-02	2.01E-03	43.5 - 44.5	6.359E-04	7.29E-05
23.5 - 24.5	4.488E-02	1.91E-03	44.5 - 45.5	1.634E-04	3.31E-05
24.5 - 25.5	4.358E-02	1.88E-03			

The flux at monoenergetic peak (36.3-45.5 MeV) is normalized to unity.
The absolute peak flux for each experiment can be obtained from Table 3.
Ratio of the peak flux to the total flux above 6.5 MeV is 1:2.17.
a Neutron flux per unit energy blow 6.5 MeV is assumed to be constant, the value between 6.5-7.5 MeV.
b Read as 4.405×10^{-2}.

Table 5 Energy spectrum of 68-MeV p-^{7}Li source neutrons.

Energy Boundary [MeV]	Flux	Error	Energy Boundary [MeV]	Flux	Error
- 6.5[a]	2.373E-02[b]		38.5 - 39.5	3.399E-02	2.10E-03
			39.5 - 40.5	3.345E-02	2.07E-03
6.5 - 7.5	2.373E-02	8.50E-04	40.5 - 41.5	3.324E-02	2.05E-03
7.5 - 8.5	2.395E-02	8.55E-04	41.5 - 42.5	3.340E-02	2.07E-03
8.5 - 9.5	2.440E-02	8.67E-04	42.5 - 43.5	3.137E-02	1.94E-03
9.5 - 10.5	2.508E-02	8.86E-04	43.5 - 44.5	3.211E-02	1.98E-03
10.5 - 11.5	2.569E-02	9.07E-04	44.5 - 45.5	3.103E-02	1.92E-03
11.5 - 12.5	2.533E-02	8.98E-04	45.5 - 46.5	3.102E-02	1.92E-03
12.5 - 13.5	2.592E-02	9.21E-04	46.5 - 47.5	3.160E-02	1.95E-03
13.5 - 14.5	2.678E-02	9.46E-04	47.5 - 48.5	3.086E-02	1.90E-03
14.5 - 15.5	2.714E-02	9.60E-04	48.5 - 49.5	3.003E-02	1.85E-03
15.5 - 16.5	2.788E-02	9.83E-04	49.5 - 50.5	2.856E-02	1.77E-03
16.5 - 17.5	2.795E-02	9.89E-04	50.5 - 51.5	2.804E-02	1.73E-03
17.5 - 18.5	2.855E-02	1.01E-03	51.5 - 52.5	2.656E-02	1.64E-03
18.5 - 19.5	2.954E-02	1.04E-03	52.5 - 53.5	2.505E-02	1.56E-03
19.5 - 20.5	3.100E-02	1.09E-03	53.5 - 54.5	2.391E-02	1.48E-03
20.5 - 21.5	3.149E-02	1.10E-03	54.5 - 55.5	2.177E-02	1.36E-03
21.5 - 22.5	3.334E-02	1.45E-03	55.5 - 56.5	1.959E-02	1.22E-03
22.5 - 23.5	3.383E-02	1.46E-03	56.5 - 57.5	1.604E-02	1.01E-03
23.5 - 24.5	3.528E-02	1.52E-03	57.5 - 58.5	1.281E-02	8.38E-04
24.5 - 25.5	3.624E-02	1.56E-03	58.5 - 59.5	1.088E-02	7.42E-04
25.5 - 26.5	3.669E-02	1.57E-03	59.5 - 60.5	9.010E-03	6.27E-04
26.5 - 27.5	3.841E-02	1.64E-03	60.5 - 61.5	7.428E-03	5.27E-04
27.5 - 28.5	3.806E-02	1.62E-03	61.5 - 62.5	8.095E-03	5.62E-04
28.5 - 29.5	3.927E-02	1.67E-03	62.5 - 63.5	4.701E-02	2.90E-03
29.5 - 30.5	3.845E-02	1.64E-03	63.5 - 64.5	2.104E-01	1.27E-02
30.5 - 31.5	3.875E-02	1.65E-03	64.5 - 65.5	3.614E-01	2.18E-02
31.5 - 32.5	3.857E-02	1.64E-03	65.5 - 66.5	2.765E-01	1.67E-02
32.5 - 33.5	3.878E-02	2.39E-03	66.5 - 67.5	8.202E-02	4.99E-03
33.5 - 34.5	3.762E-02	2.33E-03	67.5 - 68.5	8.896E-03	6.05E-04
34.5 - 35.5	3.702E-02	2.28E-03	68.5 - 69.5	1.074E-03	1.12E-04
35.5 - 36.5	3.716E-02	2.30E-03	69.5 - 70.5	4.013E-04	6.17E-05
36.5 - 37.5	3.656E-02	2.26E-03	70.5 - 71.5	4.973E-04	6.87E-05
37.5 - 38.5	3.615E-02	2.23E-03	71.5 - 72.5	1.324E-04	3.24E-05

The flux at monoenergetic peak (60.8-72.5 MeV) is normalized to unity.
The absolute peak flux for each experiment can be obtained from Table 3.
Ratio of the peak flux to the total flux above 6.5 MeV is 1:2.61.
a Neutron flux per unit energy blow 6.5 MeV is assumed to be constant, the value between 6.5-7.5 MeV.
b Read as 2.373 x 10^{-2}.

Table 6 Response functions of BC501A scintillation counter.

Group No.	Light output [MeVee]	Upper Energy Boundary of Neutron Group [MeV] 1.0	2.0	3.0	4.0	5.0	6.0	7.0	8.0	9.0
1	0.196[a]	9.54E-01[b]	5.98E-01	3.37E-01	3.33E-01	2.98E-01	2.56E-01	2.38E-01	2.86E-01	2.78E-01
2	0.543	6.05E-03	3.29E-01	3.59E-01	1.68E-01	1.01E-01	7.14E-02	6.61E-02	5.96E-02	4.87E-02
3	0.983	0.0	7.06E-03	1.88E-01	2.46E-01	1.43E-01	8.54E-02	5.96E-02	5.52E-02	4.89E-02
4	1.486	0.0	0.0	7.89E-03	1.22E-01	1.78E-01	1.15E-01	7.28E-02	5.40E-02	4.68E-02
5	2.037	0.0	0.0	0.0	8.57E-03	9.97E-02	1.34E-01	9.33E-02	6.14E-02	4.35E-02
6	2.629	0.0	0.0	0.0	0.0	1.16E-02	7.84E-02	1.03E-01	7.84E-02	5.17E-02
7	3.256	0.0	0.0	0.0	0.0	0.0	7.79E-03	6.43E-02	8.06E-02	6.50E-02
8	3.911	0.0	0.0	0.0	0.0	0.0	0.0	8.21E-03	5.08E-02	6.39E-02
9	4.590	0.0	0.0	0.0	0.0	0.0	0.0	0.0	6.36E-03	4.31E-02
10	5.287	0.0	0.0	0.0	0.0	0.0	0.0	0.0	0.0	6.87E-03
11	6.002	0.0	0.0	0.0	0.0	0.0	0.0	0.0	0.0	0.0
		Group No. 12 through 60 same as above								

a Upper group boundary of light output in MeV-electron-equivalent. Lower boundary is 0 MeVee.

b 9.54×10^{-1} [counts neutron^{-1}]

Table 6 (continued)

Group No.	Upper Light [MeVee]	Upper Energy Boundary of Neutron Group [MeV] 10.0	11.0	12.0	13.0	14.0	15.0	16.0	17.0	18.0
1	0.196	2.72E-01	2.63E-01	2.87E-01	2.78E-01	2.64E-01	2.54E-01	2.72E-01	2.70E-01	2.56E-01
2	0.543	5.20E-02	5.49E-02	5.84E-02	6.93E-02	7.60E-02	7.69E-02	7.40E-02	6.95E-02	5.80E-02
3	0.983	4.09E-02	3.35E-02	3.06E-02	3.21E-02	3.98E-02	4.37E-02	5.00E-02	5.62E-02	6.40E-02
4	1.486	4.24E-02	3.79E-02	3.13E-02	2.71E-02	2.56E-02	2.93E-02	2.89E-02	3.45E-02	3.83E-02
5	2.037	3.80E-02	3.58E-02	3.04E-02	2.56E-02	2.21E-02	2.05E-02	1.96E-02	2.02E-02	2.27E-02
6	2.629	3.69E-02	3.35E-02	2.99E-02	2.57E-02	2.21E-02	1.95E-02	1.77E-02	1.70E-02	1.62E-02
7	3.256	4.39E-02	3.41E-02	2.94E-02	2.56E-02	2.25E-02	1.99E-02	1.74E-02	1.62E-02	1.51E-02
8	3.911	5.30E-02	3.93E-02	3.04E-02	2.59E-02	2.26E-02	1.98E-02	1.72E-02	1.56E-02	1.42E-02
9	4.590	5.15E-02	4.72E-02	3.57E-02	2.74E-02	2.28E-02	2.01E-02	1.73E-02	1.56E-02	1.41E-02
10	5.287	3.52E-02	4.42E-02	4.03E-02	3.12E-02	2.40E-02	2.03E-02	1.79E-02	1.59E-02	1.43E-02
11	6.002	6.18E-03	3.13E-02	3.68E-02	3.52E-02	2.79E-02	2.21E-02	1.84E-02	1.62E-02	1.45E-02
12	6.732	0.0	6.02E-03	2.68E-02	3.19E-02	3.07E-02	2.54E-02	2.04E-02	1.71E-02	1.50E-02
13	7.476	0.0	0.0	5.48E-03	2.34E-02	2.75E-02	2.74E-02	2.32E-02	1.87E-02	1.57E-02
14	8.232	0.0	0.0	0.0	4.66E-03	1.97E-02	2.43E-02	2.38E-02	2.09E-02	1.70E-02
15	8.999	0.0	0.0	0.0	0.0	4.29E-03	1.73E-02	2.12E-02	2.13E-02	1.87E-02
16	9.776	0.0	0.0	0.0	0.0	0.0	3.78E-03	1.53E-02	1.90E-02	1.89E-02
17	10.562	0.0	0.0	0.0	0.0	0.0	0.0	3.39E-03	1.36E-02	1.71E-02
18	11.357	0.0	0.0	0.0	0.0	0.0	0.0	0.0	3.07E-03	1.22E-02
19	12.159	0.0	0.0	0.0	0.0	0.0	0.0	0.0	0.0	2.90E-03
20	12.968	0.0	0.0	0.0	0.0	0.0	0.0	0.0	0.0	0.0
		Group No. 21 through 60 same as above								

Table 6 (continued)

Group No.	Upper Light [MeVee]	Upper Energy Boundary of Neutron Group [MeV] 19.0	20.0	21.0	22.0	23.0	24.0	25.0	26.0	27.0
1	0.196	2.65E-01	2.72E-01	2.70E-01	2.63E-01	2.65E-01	2.65E-01	2.68E-01	2.69E-01	2.69E-01
2	0.543	4.06E-02	3.97E-02	3.24E-02	2.90E-02	2.46E-02	2.17E-02	2.02E-02	1.85E-02	1.76E-02
3	0.983	6.77E-02	5.43E-02	4.57E-02	3.43E-02	2.74E-02	2.44E-02	2.05E-02	1.81E-02	1.69E-02
4	1.486	4.75E-02	4.62E-02	5.31E-02	5.48E-02	4.75E-02	3.81E-02	3.16E-02	2.68E-02	2.47E-02
5	2.037	2.52E-02	3.07E-02	3.11E-02	3.58E-02	3.88E-02	3.96E-02	3.95E-02	3.26E-02	2.71E-02
6	2.629	1.73E-02	1.86E-02	2.32E-02	2.29E-02	2.31E-02	2.40E-02	2.74E-02	2.89E-02	2.93E-02
7	3.256	1.45E-02	1.48E-02	1.49E-02	1.71E-02	1.90E-02	1.96E-02	1.84E-02	1.85E-02	2.01E-02
8	3.911	1.33E-02	1.24E-02	1.25E-02	1.22E-02	1.40E-02	1.56E-02	1.53E-02	1.54E-02	1.45E-02
9	4.590	1.30E-02	1.17E-02	1.07E-02	1.10E-02	1.11E-02	1.25E-02	1.26E-02	1.19E-02	1.28E-02
10	5.287	1.29E-02	1.14E-02	1.03E-02	9.98E-03	1.02E-02	1.01E-02	1.04E-02	1.13E-02	1.08E-02
11	6.002	1.28E-02	1.15E-02	1.01E-02	9.54E-03	8.87E-03	9.29E-03	8.85E-03	9.19E-03	1.05E-02
12	6.732	1.38E-02	1.17E-02	1.05E-02	9.46E-03	8.71E-03	8.31E-03	8.80E-03	8.65E-03	8.66E-03
13	7.476	1.40E-02	1.25E-02	1.06E-02	9.50E-03	8.80E-03	8.07E-03	7.66E-03	8.23E-03	8.01E-03
14	8.232	1.45E-02	1.23E-02	1.09E-02	9.82E-03	8.86E-03	8.01E-03	7.45E-03	6.89E-03	7.38E-03
15	8.999	1.54E-02	1.31E-02	1.12E-02	1.00E-02	8.91E-03	7.97E-03	7.38E-03	6.62E-03	6.31E-03
16	9.776	1.72E-02	1.41E-02	1.14E-02	1.02E-02	9.18E-03	8.18E-03	7.42E-03	6.77E-03	6.31E-03
17	10.562	1.75E-02	1.51E-02	1.27E-02	1.09E-02	9.24E-03	8.38E-03	7.46E-03	6.87E-03	6.04E-03
18	11.357	1.56E-02	1.54E-02	1.41E-02	1.16E-02	9.76E-03	8.52E-03	7.58E-03	6.76E-03	6.18E-03
19	12.159	1.08E-02	1.39E-02	1.37E-02	1.28E-02	1.10E-02	9.00E-03	7.95E-03	6.95E-03	6.24E-03
20	12.968	2.64E-03	9.60E-03	1.24E-02	1.26E-02	1.17E-02	9.80E-03	8.59E-03	7.48E-03	6.41E-03
21	13.787	0.0	2.32E-03	8.42E-03	1.14E-02	1.13E-02	1.07E-02	9.27E-03	7.54E-03	6.72E-03
22	14.606	0.0	0.0	2.09E-03	7.62E-03	1.04E-02	1.02E-02	9.68E-03	8.12E-03	7.31E-03
23	15.436	0.0	0.0	0.0	1.89E-03	6.69E-03	9.31E-03	9.13E-03	8.90E-03	7.74E-03
24	16.266	0.0	0.0	0.0	0.0	1.74E-03	5.88E-03	8.58E-03	8.29E-03	8.00E-03
25	17.106	0.0	0.0	0.0	0.0	0.0	1.43E-03	5.20E-03	7.75E-03	7.84E-03
26	17.946	0.0	0.0	0.0	0.0	0.0	0.0	1.23E-03	4.68E-03	7.00E-03
27	18.795	0.0	0.0	0.0	0.0	0.0	0.0	0.0	1.13E-03	3.94E-03
28	19.641	0.0	0.0	0.0	0.0	0.0	0.0	0.0	0.0	1.02E-03
29	20.484	0.0	0.0	0.0	0.0	0.0	0.0	0.0	0.0	0.0
		Group No. 30 through 60 same as above								

Table 6 (continued)

Group No.	Light output [MeVee]	Upper Energy Boundary of Neutron Group [MeV] 28.0	29.0	30.0	31.0	32.0	33.0	34.0	35.0	36.0
1	0.196	2.67E-01	2.69E-01	2.78E-01	2.69E-01	2.67E-01	2.67E-01	2.65E-01	2.63E-01	2.63E-01
2	0.543	1.62E-02	1.50E-02	1.46E-02	1.39E-02	1.32E-02	1.17E-02	1.15E-02	1.09E-02	1.03E-02
3	0.983	1.61E-02	1.53E-02	1.45E-02	1.45E-02	1.38E-02	1.28E-02	1.25E-02	1.16E-02	1.07E-02
4	1.486	2.29E-02	2.20E-02	2.10E-02	2.02E-02	2.04E-02	1.94E-02	1.29E-02	1.26E-02	1.16E-02
5	2.037	2.28E-02	1.96E-02	1.82E-02	1.69E-02	1.63E-02	1.53E-02	1.38E-02	1.34E-02	1.30E-02
6	2.629	2.64E-02	2.32E-02	1.96E-02	1.65E-02	1.52E-02	1.39E-02	1.31E-02	1.27E-02	1.30E-02
7	3.256	2.16E-02	2.20E-02	2.08E-02	1.91E-02	1.69E-02	1.46E-02	1.39E-02	1.24E-02	1.27E-02
8	3.911	1.47E-02	1.57E-02	1.66E-02	1.64E-02	1.58E-02	1.45E-02	1.40E-02	1.37E-02	1.28E-02
9	4.590	1.30E-02	1.25E-02	1.26E-02	1.23E-02	1.25E-02	1.25E-02	1.22E-02	1.21E-02	1.21E-02
10	5.287	1.07E-02	1.11E-02	1.10E-02	1.07E-02	9.88E-03	9.94E-03	9.82E-03	1.04E-02	1.03E-02
11	6.002	1.02E-02	1.01E-02	9.66E-03	9.68E-03	9.99E-03	8.90E-03	8.80E-03	8.55E-03	9.29E-03
12	6.732	9.77E-03	9.68E-03	9.65E-03	9.33E-03	8.89E-03	8.48E-03	8.50E-03	8.30E-03	8.34E-03
13	7.476	7.88E-03	9.77E-03	9.63E-03	8.92E-03	8.55E-03	8.39E-03	7.86E-03	7.66E-03	7.85E-03
14	8.232	7.25E-03	7.35E-03	9.21E-03	8.73E-03	8.66E-03	8.08E-03	7.63E-03	7.53E-03	7.54E-03
15	8.999	6.80E-03	6.78E-03	6.77E-03	8.09E-03	8.53E-03	7.56E-03	7.62E-03	7.14E-03	7.48E-03
16	9.776	5.84E-03	6.33E-03	6.27E-03	5.96E-03	7.52E-03	8.05E-03	7.57E-03	7.29E-03	7.26E-03
17	10.562	5.60E-03	5.41E-03	5.99E-03	5.80E-03	5.49E-03	6.60E-03	7.91E-03	7.05E-03	7.56E-03
18	11.357	5.56E-03	5.34E-03	5.13E-03	5.77E-03	5.34E-03	5.15E-03	6.11E-03	7.21E-03	7.45E-03
19	12.159	5.52E-03	5.27E-03	4.86E-03	4.90E-03	5.29E-03	5.14E-03	4.58E-03	5.41E-03	6.96E-03
20	12.968	5.67E-03	5.28E-03	4.84E-03	4.53E-03	4.57E-03	4.80E-03	4.54E-03	4.42E-03	5.06E-03
21	13.787	6.06E-03	5.45E-03	5.15E-03	4.50E-03	4.23E-03	4.02E-03	4.16E-03	4.32E-03	4.15E-03
22	14.606	6.19E-03	5.70E-03	5.06E-03	4.71E-03	4.21E-03	3.98E-03	3.72E-03	4.00E-03	4.06E-03
23	15.436	6.69E-03	5.69E-03	5.33E-03	4.70E-03	4.29E-03	3.84E-03	3.65E-03	3.60E-03	3.81E-03
24	16.266	7.06E-03	6.16E-03	5.58E-03	4.80E-03	4.50E-03	4.17E-03	3.62E-03	3.48E-03	3.42E-03
25	17.106	7.36E-03	6.76E-03	5.83E-03	5.02E-03	4.74E-03	4.35E-03	3.66E-03	3.48E-03	3.32E-03
26	17.946	6.90E-03	6.77E-03	6.15E-03	5.57E-03	4.95E-03	4.35E-03	3.77E-03	3.59E-03	3.25E-03
27	18.795	6.37E-03	6.75E-03	6.37E-03	6.02E-03	4.93E-03	4.45E-03	3.87E-03	3.64E-03	3.38E-03
28	19.641	3.37E-03	5.89E-03	6.33E-03	5.81E-03	5.58E-03	4.54E-03	4.09E-03	3.74E-03	3.39E-03
29	20.484	8.82E-04	3.13E-03	5.57E-03	5.57E-03	5.29E-03	4.95E-03	4.34E-03	3.93E-03	3.53E-03
30	21.329	0.0	8.64E-04	2.84E-03	4.74E-03	5.32E-03	4.91E-03	4.59E-03	4.16E-03	3.71E-03
31	22.177	0.0	0.0	7.03E-04	2.58E-03	4.42E-03	4.78E-03	4.65E-03	4.39E-03	3.90E-03
32	23.026	0.0	0.0	0.0	6.55E-04	2.12E-03	4.08E-03	4.57E-03	4.39E-03	4.14E-03
33	23.875	0.0	0.0	0.0	0.0	5.89E-04	2.11E-03	4.00E-03	4.32E-03	4.17E-03
34	24.727	0.0	0.0	0.0	0.0	0.0	4.91E-04	2.47E-03	3.84E-03	4.14E-03
35	25.577	0.0	0.0	0.0	0.0	0.0	0.0	9.71E-04	2.42E-03	3.66E-03
36	26.426	0.0	0.0	0.0	0.0	0.0	0.0	0.0	9.84E-04	2.30E-03
37	27.274	0.0	0.0	0.0	0.0	0.0	0.0	0.0	0.0	9.30E-04
38	28.120	0.0	0.0	0.0	0.0	0.0	0.0	0.0	0.0	0.0
		Group No. 39 through 60 same as above								

Table 6 (continued)

Group No.	Upper Light [MeVee]	Upper Energy Boundary of Neutron Group [MeV] 37.0	38.0	39.0	40.0	41.0	42.0	43.0	44.0	46.0
1	0.196	2.60E-01	2.59E-01	2.58E-01	2.56E-01	2.54E-01	2.52E-01	2.50E-01	2.48E-01	2.44E-01
2	0.543	9.48E-03	8.89E-03	7.90E-03	8.51E-03	7.78E-03	7.61E-03	7.09E-03	7.12E-03	6.46E-03
3	0.983	1.03E-02	9.36E-03	8.80E-03	9.14E-03	8.57E-03	8.74E-03	7.99E-03	7.86E-03	7.32E-03
4	1.486	1.14E-02	1.03E-02	9.77E-03	9.17E-03	8.78E-03	8.45E-03	8.11E-03	7.91E-03	7.35E-03
5	2.037	1.26E-02	1.17E-02	1.15E-02	1.06E-02	1.05E-02	9.22E-03	8.92E-03	8.15E-03	7.50E-03
6	2.629	1.30E-02	1.21E-02	1.28E-02	1.17E-02	1.11E-02	1.08E-02	1.04E-02	9.75E-03	8.89E-03
7	3.256	1.18E-02	1.12E-02	1.17E-02	1.13E-02	1.12E-02	1.14E-02	1.04E-02	9.93E-03	9.19E-03
8	3.911	1.18E-02	1.12E-02	1.05E-02	1.04E-02	1.03E-02	1.00E-02	9.65E-03	9.34E-03	9.00E-03
9	4.590	1.18E-02	1.11E-02	1.13E-02	1.03E-02	9.52E-03	9.21E-03	8.99E-03	8.74E-03	8.33E-03
10	5.287	1.03E-02	1.01E-02	1.08E-02	1.03E-02	9.65E-03	9.35E-03	8.08E-03	8.09E-03	7.70E-03
11	6.002	8.91E-03	8.43E-03	8.99E-03	8.89E-03	9.13E-03	8.69E-03	8.41E-03	8.19E-03	7.42E-03
12	6.732	7.57E-03	7.20E-03	8.01E-03	7.81E-03	8.13E-03	7.95E-03	8.02E-03	8.03E-03	7.45E-03
13	7.476	7.53E-03	7.09E-03	6.96E-03	6.40E-03	6.74E-03	6.86E-03	6.94E-03	7.14E-03	7.12E-03
14	8.232	7.38E-03	6.75E-03	6.84E-03	6.29E-03	6.07E-03	6.08E-03	6.00E-03	6.20E-03	6.47E-03
15	8.999	6.72E-03	6.33E-03	6.65E-03	6.71E-03	5.86E-03	6.00E-03	5.41E-03	5.37E-03	5.71E-03
16	9.776	6.90E-03	6.53E-03	6.23E-03	6.16E-03	5.82E-03	5.73E-03	5.46E-03	5.18E-03	5.17E-03
17	10.562	6.80E-03	6.20E-03	6.43E-03	5.94E-03	5.63E-03	5.10E-03	5.21E-03	5.02E-03	4.72E-03
18	11.357	6.76E-03	6.46E-03	6.12E-03	5.77E-03	5.43E-03	5.66E-03	5.05E-03	5.10E-03	4.51E-03
19	12.159	6.58E-03	6.32E-03	6.02E-03	5.61E-03	5.46E-03	5.10E-03	4.75E-03	4.48E-03	4.15E-03
20	12.968	6.35E-03	6.49E-03	6.24E-03	5.66E-03	5.46E-03	5.26E-03	4.68E-03	4.37E-03	4.15E-03
21	13.787	4.66E-03	6.28E-03	6.43E-03	5.87E-03	5.45E-03	5.31E-03	4.79E-03	4.53E-03	4.18E-03
22	14.606	3.75E-03	4.40E-03	5.92E-03	6.15E-03	5.82E-03	5.35E-03	4.96E-03	4.61E-03	4.17E-03
23	15.436	3.79E-03	3.68E-03	4.20E-03	5.53E-03	6.16E-03	5.66E-03	5.15E-03	4.65E-03	4.27E-03
24	16.266	3.53E-03	3.58E-03	3.45E-03	3.86E-03	5.32E-03	5.80E-03	5.34E-03	4.92E-03	4.44E-03
25	17.106	3.15E-03	3.42E-03	3.53E-03	3.29E-03	3.65E-03	4.99E-03	5.64E-03	5.20E-03	4.62E-03
26	17.946	2.96E-03	3.08E-03	3.28E-03	3.28E-03	3.17E-03	3.51E-03	4.61E-03	5.31E-03	4.86E-03
27	18.795	3.06E-03	2.85E-03	3.00E-03	3.07E-03	3.08E-03	3.00E-03	3.27E-03	4.19E-03	4.99E-03
28	19.641	3.00E-03	2.92E-03	2.82E-03	2.79E-03	2.87E-03	2.97E-03	2.77E-03	2.97E-03	4.38E-03
29	20.484	3.11E-03	2.94E-03	2.78E-03	2.59E-03	2.61E-03	2.77E-03	2.69E-03	2.57E-03	3.26E-03
30	21.329	3.27E-03	3.02E-03	2.81E-03	2.61E-03	2.46E-03	2.49E-03	2.58E-03	2.56E-03	2.55E-03
31	22.177	3.41E-03	3.16E-03	2.92E-03	2.69E-03	2.52E-03	2.37E-03	2.31E-03	2.38E-03	2.40E-03
32	23.026	3.65E-03	3.31E-03	3.02E-03	2.69E-03	2.45E-03	2.38E-03	2.21E-03	2.21E-03	2.40E-03
33	23.875	3.83E-03	3.44E-03	3.16E-03	2.78E-03	2.61E-03	2.42E-03	2.13E-03	2.11E-03	2.16E-03
34	24.727	3.81E-03	3.68E-03	3.31E-03	2.98E-03	2.71E-03	2.56E-03	2.23E-03	2.06E-03	2.01E-03
35	25.577	3.81E-03	3.64E-03	3.45E-03	3.18E-03	2.93E-03	2.62E-03	2.38E-03	2.13E-03	1.91E-03
36	26.426	3.34E-03	3.57E-03	3.50E-03	3.10E-03	2.94E-03	2.72E-03	2.39E-03	2.14E-03	1.93E-03
37	27.274	2.07E-03	3.20E-03	3.49E-03	3.27E-03	3.07E-03	2.78E-03	2.42E-03	2.24E-03	2.01E-03
38	28.120	8.64E-04	1.96E-03	3.05E-03	3.22E-03	3.13E-03	2.89E-03	2.63E-03	2.33E-03	2.01E-03
39	28.966	0.0	8.34E-04	1.85E-03	2.74E-03	3.11E-03	2.96E-03	2.65E-03	2.47E-03	2.08E-03
40	29.809	0.0	0.0	7.82E-04	1.74E-03	2.67E-03	2.98E-03	2.71E-03	2.52E-03	2.18E-03
41	30.651	0.0	0.0	0.0	7.73E-04	1.63E-03	2.46E-03	2.76E-03	2.54E-03	2.30E-03
42	31.491	0.0	0.0	0.0	0.0	7.25E-04	1.53E-03	2.31E-03	2.57E-03	2.38E-03
43	32.328	0.0	0.0	0.0	0.0	0.0	7.12E-04	1.50E-03	2.15E-03	2.31E-03
44	33.162	0.0	0.0	0.0	0.0	0.0	0.0	6.38E-04	1.35E-03	2.15E-03
45	34.822	0.0	0.0	0.0	0.0	0.0	0.0	0.0	8.31E-04	2.42E-03
46	36.473	0.0	0.0	0.0	0.0	0.0	0.0	0.0	0.0	5.03E-04
47	38.113	0.0	0.0	0.0	0.0	0.0	0.0	0.0	0.0	0.0
		Group No. 48 through 60 same as above								

Table 6 (continued)

Group No.	Upper Light [MeVee]	Upper Energy Boundary of Neutron Group [MeV] 48.0	50.0	52.0	54.0	56.0	58.0	60.0	62.0	64.0
1	0.196	2.36E-01	2.28E-01	2.22E-01	2.19E-01	2.15E-01	2.09E-01	2.03E-01	1.97E-01	1.92E-01
2	0.543	5.81E-03	5.61E-03	5.22E-03	5.01E-03	4.69E-03	4.42E-03	4.09E-03	3.94E-03	3.97E-03
3	0.983	6.63E-03	6.24E-03	5.86E-03	5.39E-03	5.14E-03	4.93E-03	4.43E-03	4.32E-03	4.24E-03
4	1.486	6.74E-03	6.58E-03	5.90E-03	5.54E-03	5.34E-03	5.15E-03	4.67E-03	4.56E-03	4.52E-03
5	2.037	6.78E-03	6.38E-03	5.80E-03	5.41E-03	5.25E-03	4.88E-03	4.70E-03	4.50E-03	4.29E-03
6	2.629	8.42E-03	7.42E-03	6.52E-03	5.88E-03	5.66E-03	3.84E-03	4.71E-03	4.43E-03	4.05E-03
7	3.256	8.47E-03	7.24E-03	6.73E-03	5.87E-03	5.75E-03	5.14E-03	4.71E-03	4.38E-03	3.92E-03
8	3.911	8.81E-03	7.29E-03	6.34E-03	5.86E-03	5.64E-03	5.20E-03	4.78E-03	4.36E-03	4.04E-03
9	4.590	8.16E-03	7.22E-03	6.40E-03	5.79E-03	5.49E-03	5.00E-03	4.63E-03	4.27E-03	3.81E-03
10	5.287	7.65E-03	6.98E-03	6.11E-03	5.82E-03	5.45E-03	4.97E-03	4.52E-03	4.05E-03	3.67E-03
11	6.002	7.48E-03	6.37E-03	5.67E-03	5.23E-03	5.29E-03	5.26E-03	4.34E-03	3.90E-03	3.64E-03
12	6.732	6.84E-03	6.16E-03	5.56E-03	5.46E-03	5.27E-03	4.87E-03	4.08E-03	3.75E-03	3.48E-03
13	7.476	6.95E-03	5.87E-03	5.58E-03	5.10E-03	5.17E-03	5.17E-03	4.35E-03	3.85E-03	3.50E-03
14	8.232	6.43E-03	5.95E-03	5.21E-03	5.11E-03	4.73E-03	4.83E-03	4.29E-03	3.88E-03	3.43E-03
15	8.999	6.19E-03	5.58E-03	5.19E-03	4.50E-03	4.62E-03	4.34E-03	4.27E-03	3.88E-03	3.28E-03
16	9.776	5.25E-03	5.20E-03	4.85E-03	4.81E-03	4.37E-03	4.44E-03	4.13E-03	3.74E-03	3.28E-03
17	10.562	5.17E-03	4.78E-03	4.75E-03	4.79E-03	4.83E-03	4.33E-03	3.73E-03	3.60E-03	3.35E-03
18	11.357	4.57E-03	4.27E-03	4.39E-03	4.03E-03	4.18E-03	4.35E-03	3.78E-03	3.51E-03	3.29E-03
19	12.159	4.13E-03	3.94E-03	3.95E-03	3.92E-03	4.04E-03	3.71E-03	3.69E-03	3.45E-03	3.26E-03
20	12.968	3.84E-03	3.70E-03	3.68E-03	3.51E-03	3.64E-03	3.57E-03	3.61E-03	3.37E-03	3.14E-03
21	13.787	3.83E-03	3.41E-03	3.47E-03	3.39E-03	3.43E-03	3.53E-03	3.53E-03	3.24E-03	3.10E-03
22	14.606	3.80E-03	3.35E-03	3.25E-03	3.26E-03	3.26E-03	3.27E-03	3.25E-03	3.11E-03	2.94E-03
23	15.436	3.90E-03	3.41E-03	3.08E-03	3.12E-03	3.19E-03	3.09E-03	3.11E-03	3.17E-03	2.98E-03
24	16.266	3.94E-03	3.30E-03	3.07E-03	2.85E-03	2.92E-03	3.03E-03	3.03E-03	2.89E-03	2.88E-03
25	17.106	4.09E-03	3.36E-03	3.13E-03	2.81E-03	2.74E-03	2.81E-03	3.09E-03	2.84E-03	2.67E-03
26	17.946	4.21E-03	3.55E-03	3.07E-03	2.82E-03	2.71E-03	2.75E-03	2.76E-03	2.78E-03	2.53E-03
27	18.795	4.36E-03	3.53E-03	3.16E-03	2.79E-03	2.65E-03	2.65E-03	2.59E-03	2.63E-03	2.49E-03
28	19.641	4.63E-03	3.70E-03	3.31E-03	2.92E-03	2.57E-03	2.37E-03	2.42E-03	2.59E-03	2.38E-03
29	20.484	4.59E-03	3.98E-03	3.24E-03	2.75E-03	2.63E-03	2.39E-03	2.16E-03	2.31E-03	2.24E-03
30	21.329	3.99E-03	4.18E-03	3.49E-03	2.79E-03	2.52E-03	2.43E-03	2.23E-03	2.21E-03	2.16E-03
31	22.177	2.98E-03	4.10E-03	3.74E-03	2.96E-03	2.65E-03	2.38E-03	2.42E-03	1.99E-03	2.12E-03
32	23.026	2.40E-03	3.52E-03	3.98E-03	3.32E-03	2.69E-03	2.41E-03	2.24E-03	2.13E-03	1.99E-03
33	23.875	2.26E-03	2.56E-03	3.84E-03	3.46E-03	2.85E-03	2.42E-03	2.23E-03	1.93E-03	1.79E-03
34	24.727	2.13E-03	1.98E-03	3.17E-03	3.69E-03	3.13E-03	2.46E-03	2.36E-03	2.00E-03	1.90E-03
35	25.577	1.97E-03	1.91E-03	2.33E-03	3.34E-03	3.38E-03	2.71E-03	2.30E-03	2.03E-03	1.75E-03
36	26.426	1.80E-03	1.85E-03	1.94E-03	2.70E-03	3.48E-03	2.84E-03	2.35E-03	2.11E-03	1.77E-03
37	27.274	1.78E-03	1.75E-03	1.76E-03	2.05E-03	3.20E-03	3.18E-03	2.63E-03	2.15E-03	1.85E-03
38	28.120	1.70E-03	1.60E-03	1.72E-03	1.63E-03	2.50E-03	3.13E-03	2.72E-03	2.28E-03	1.86E-03
39	28.966	1.81E-03	1.48E-03	1.58E-03	1.58E-03	1.83E-03	2.90E-03	2.99E-03	2.20E-03	2.01E-03
40	29.809	1.86E-03	1.51E-03	1.45E-03	1.51E-03	1.59E-03	2.30E-03	3.01E-03	2.60E-03	2.03E-03
41	30.651	2.00E-03	1.58E-03	1.42E-03	1.40E-03	1.48E-03	1.61E-03	2.34E-03	2.75E-03	2.18E-03
42	31.491	2.04E-03	1.64E-03	1.40E-03	1.27E-03	1.35E-03	1.42E-03	1.70E-03	2.51E-03	2.41E-03
43	32.328	2.15E-03	1.65E-03	1.37E-03	1.26E-03	1.28E-03	1.41E-03	1.28E-03	1.99E-03	2.48E-03
44	33.162	2.15E-03	1.78E-03	1.49E-03	1.28E-03	1.19E-03	1.31E-03	1.22E-03	1.35E-03	2.19E-03
45	34.822	4.03E-03	3.72E-03	3.14E-03	2.52E-03	2.26E-03	2.26E-03	2.27E-03	2.23E-03	2.90E-03
46	36.473	2.24E-03	3.50E-03	3.28E-03	2.74E-03	2.34E-03	2.14E-03	2.09E-03	1.98E-03	2.12E-03
47	38.113	4.85E-04	1.92E-03	3.20E-03	2.98E-03	2.55E-03	2.13E-03	1.92E-03	1.81E-03	1.88E-03
48	39.742	0.0	4.43E-04	1.73E-03	2.88E-03	2.75E-03	2.36E-03	1.98E-03	1.69E-03	1.46E-03
49	41.365	0.0	0.0	3.95E-04	1.53E-03	2.61E-03	2.57E-03	2.15E-03	1.79E-03	1.56E-03
50	42.983	0.0	0.0	0.0	3.57E-04	1.41E-03	2.32E-03	2.23E-03	1.93E-03	1.60E-03
51	44.592	0.0	0.0	0.0	0.0	3.12E-04	1.23E-03	2.10E-03	2.00E-03	1.83E-03
52	46.194	0.0	0.0	0.0	0.0	0.0	2.51E-04	1.08E-03	2.01E-03	1.79E-03
53	47.788	0.0	0.0	0.0	0.0	0.0	0.0	2.07E-04	9.47E-04	1.72E-03
54	49.372	0.0	0.0	0.0	0.0	0.0	0.0	0.0	2.50E-04	8.56E-04
55	50.948	0.0	0.0	0.0	0.0	0.0	0.0	0.0	0.0	2.03E-04
56	52.518	0.0	0.0	0.0	0.0	0.0	0.0	0.0	0.0	0.0
		Group No. 57 through 60 same as above								

Table 6 (continued)

Group No.	Upper Light [MeVee]	Upper Energy Boundary of Neutron Group [MeV] 66.0	68.0	70.0	74.0	78.0
1	0.196	1.87E-01	1.82E-01	1.78E-01	1.70E-01	1.62E-01
2	0.543	3.70E-03	3.53E-03	3.42E-03	3.28E-03	3.02E-03
3	0.983	3.98E-03	3.48E-03	3.52E-03	3.20E-03	3.01E-03
4	1.486	4.05E-03	3.77E-03	3.70E-03	3.29E-03	3.16E-03
5	2.037	4.05E-03	3.75E-03	3.74E-03	3.23E-03	2.99E-03
6	2.629	3.95E-03	3.65E-03	3.57E-03	3.30E-03	3.13E-03
7	3.256	3.78E-03	3.72E-03	3.34E-03	3.14E-03	2.69E-03
8	3.911	3.83E-03	3.76E-03	3.53E-03	3.17E-03	2.70E-03
9	4.590	3.78E-03	3.74E-03	3.71E-03	3.43E-03	2.97E-03
10	5.287	3.77E-03	3.53E-03	3.50E-03	3.23E-03	2.80E-03
11	6.002	3.58E-03	3.36E-03	3.52E-03	3.22E-03	2.72E-03
12	6.732	3.54E-03	3.24E-03	3.42E-03	3.14E-03	2.49E-03
13	7.476	3.44E-03	3.39E-03	3.40E-03	3.07E-03	2.64E-03
14	8.232	3.37E-03	3.20E-03	3.28E-03	3.05E-03	2.51E-03
15	8.999	3.27E-03	3.30E-03	3.23E-03	2.95E-03	2.50E-03
16	9.776	3.30E-03	3.15E-03	3.30E-03	2.98E-03	2.47E-03
17	10.562	3.44E-03	3.04E-03	3.30E-03	2.90E-03	2.33E-03
18	11.357	3.29E-03	3.26E-03	3.11E-03	2.90E-03	2.41E-03
19	12.159	3.21E-03	3.22E-03	3.34E-03	2.79E-03	2.32E-03
20	12.968	3.19E-03	3.14E-03	3.11E-03	2.73E-03	2.34E-03
21	13.787	2.98E-03	2.94E-03	3.10E-03	2.73E-03	2.34E-03
22	14.606	2.94E-03	2.89E-03	3.08E-03	2.73E-03	2.36E-03
23	15.436	2.86E-03	3.05E-03	3.10E-03	2.67E-03	2.22E-03
24	16.266	2.83E-03	2.91E-03	2.85E-03	2.63E-03	2.25E-03
25	17.106	2.78E-03	2.74E-03	2.70E-03	2.53E-03	2.17E-03
26	17.946	2.67E-03	2.75E-03	2.79E-03	2.56E-03	2.18E-03
27	18.795	2.56E-03	2.77E-03	2.75E-03	2.59E-03	2.18E-03
28	19.641	2.54E-03	2.42E-03	2.70E-03	2.42E-03	2.09E-03
29	20.484	2.45E-03	2.30E-03	2.42E-03	2.38E-03	2.01E-03
30	21.329	2.36E-03	2.30E-03	2.50E-03	2.32E-03	2.11E-03
31	22.177	2.08E-03	2.08E-03	2.44E-03	2.33E-03	2.00E-03
32	23.026	2.04E-03	2.17E-03	2.31E-03	2.18E-03	1.98E-03
33	23.875	2.04E-03	2.08E-03	2.26E-03	2.03E-03	1.87E-03
34	24.727	1.80E-03	1.80E-03	2.15E-03	1.93E-03	1.80E-03
35	25.577	1.77E-03	1.78E-03	2.03E-03	1.92E-03	1.68E-03
36	26.426	1.92E-03	1.84E-03	2.07E-03	1.80E-03	1.63E-03
37	27.274	1.78E-03	1.67E-03	1.83E-03	1.78E-03	1.62E-03
38	28.120	1.74E-03	1.74E-03	1.74E-03	1.74E-03	1.53E-03
39	28.966	1.73E-03	1.67E-03	1.72E-03	1.60E-03	1.60E-03
40	29.809	1.80E-03	1.68E-03	1.76E-03	1.55E-03	1.53E-03
41	30.651	1.94E-03	1.66E-03	1.57E-03	1.48E-03	1.46E-03
42	31.491	2.07E-03	1.76E-03	1.70E-03	1.48E-03	1.37E-03
43	32.328	2.26E-03	1.78E-03	1.77E-03	1.37E-03	1.32E-03
44	33.162	2.41E-03	1.83E-03	1.64E-03	1.36E-03	1.31E-03
45	34.822	4.57E-03	4.29E-03	3.68E-03	2.91E-03	2.41E-03
46	36.473	2.83E-03	4.07E-03	4.52E-03	3.02E-03	2.22E-03
47	38.113	1.98E-03	2.56E-03	3.97E-03	3.57E-03	2.25E-03
48	39.742	1.83E-03	1.91E-03	2.65E-03	3.57E-03	2.46E-03
49	41.365	1.58E-03	1.58E-03	1.85E-03	2.77E-03	2.85E-03
50	42.983	1.47E-03	1.45E-03	1.62E-03	1.85E-03	2.90E-03
51	44.592	1.57E-03	1.32E-03	1.39E-03	1.48E-03	2.11E-03
52	46.194	1.59E-03	1.53E-03	1.22E-03	1.32E-03	1.42E-03
53	47.788	1.72E-03	1.49E-03	1.39E-03	1.19E-03	1.18E-03
54	49.372	1.59E-03	1.58E-03	1.46E-03	1.21E-03	1.04E-03
55	50.948	7.69E-04	1.49E-03	1.55E-03	1.28E-03	1.01E-03
56	52.518	1.72E-04	7.62E-04	1.44E-03	1.27E-03	9.18E-04
57	54.079	0.0	1.62E-04	7.63E-04	1.29E-03	9.72E-04
58	57.171	0.0	0.0	2.17E-04	1.35E-03	2.16E-03
59	60.225	0.0	0.0	0.0	1.30E-04	1.04E-03
60	63.249	0.0	0.0	0.0	0.0	9.24E-05

Table 7 Response functions of Bonner ball counter.

Upper Energy Boundary [eV]	Response [counts neutron^{-1} cm^2]				
	Bare [a]	1.5cm [b]	3.0cm	5.0cm	9.0cm
4.00E+08 [c]	0.000E+00	7.500E-03	6.624E-02	2.465E-01	7.141E-01
3.50E+08	0.000E+00	7.603E-03	6.710E-02	2.492E-01	7.189E-01
3.00E+08	0.000E+00	8.210E-03	7.326E-02	2.737E-01	7.905E-01
2.50E+08	0.000E+00	8.831E-03	7.866E-02	2.934E-01	8.440E-01
2.00E+08	0.000E+00	9.648E-03	8.484E-02	3.132E-01	8.910E-01
1.60E+08	0.000E+00	1.110E-02	9.654E-02	3.529E-01	9.907E-01
1.20E+08	0.000E+00	1.280E-02	1.104E-01	3.998E-01	1.107E+00
1.00E+08	0.000E+00	1.425E-02	1.226E-01	4.425E-01	1.216E+00
8.00E+07	0.000E+00	1.565E-02	1.349E-01	4.868E-01	1.332E+00
6.50E+07	0.000E+00	1.702E-02	1.468E-01	5.296E-01	1.443E+00
5.50E+07	0.000E+00	1.809E-02	1.560E-01	5.623E-01	1.527E+00
4.50E+07	0.000E+00	1.957E-02	1.690E-01	6.106E-01	1.658E+00
3.50E+07	3.089E-03	2.312E-02	1.995E-01	7.198E-01	1.941E+00
2.75E+07	7.928E-03	2.808E-02	2.409E-01	8.650E-01	2.298E+00
2.25E+07	1.133E-02	3.749E-02	3.165E-01	1.115E+00	2.856E+00
1.75E+07	1.730E-02	5.766E-02	4.246E-01	1.438E+00	3.486E+00
1.35E+07	2.313E-02	8.420E-02	5.348E-01	1.758E+00	4.099E+00
1.00E+07	3.072E-02	1.239E-01	7.926E-01	2.498E+00	5.327E+00
6.70E+06	3.902E-02	2.010E-01	1.273E+00	3.721E+00	6.945E+00
4.49E+06	4.692E-02	3.001E-01	1.830E+00	4.882E+00	7.672E+00
3.01E+06	5.285E-02	4.456E-01	2.587E+00	6.317E+00	8.514E+00
2.02E+06	5.474E-02	6.413E-01	3.482E+00	7.721E+00	8.768E+00
1.35E+06	3.315E-02	8.836E-01	4.420E+00	8.785E+00	8.184E+00
9.07E+05	1.558E-02	1.276E+00	5.539E+00	9.560E+00	6.953E+00
4.98E+05	1.831E-02	1.941E+00	6.808E+00	9.768E+00	5.165E+00
2.24E+05	2.814E-02	2.779E+00	7.765E+00	9.243E+00	3.613E+00
8.65E+04	6.642E-02	3.874E+00	8.481E+00	8.393E+00	2.574E+00
1.50E+04	1.616E-01	5.194E+00	9.251E+00	7.861E+00	2.044E+00
3.35E+03	4.011E-01	6.778E+00	1.001E+01	7.479E+00	1.740E+00
4.54E+02	1.572E+00	9.425E+00	1.066E+01	6.709E+00	1.381E+00
2.26E+01	4.537E+00	1.208E+01	1.040E+01	5.536E+00	1.036E+00
5.04E+00	9.596E+00	1.275E+01	9.083E+00	4.437E+00	8.043E-01
1.12E+00	1.759E+01	1.143E+01	6.992E+00	3.254E+00	5.812E-01
4.14E-01	1.881E+01	4.797E+00	2.607E+00	1.190E+00	2.193E-01
1.00E-04					

a ^{3}He counter (10 atm)

b Thickness of polyethylene moderator

c Read as 4.00 x 10^8

Table 8 Fission cross sections of ^{232}Th and ^{238}U.

Upper Energy Boundary [eV]	Cross Section [barn]		Upper Energy Boundary [eV]	Cross Section [barn]	
	^{232}Th	^{238}U		^{232}Th	^{238}U
4.00E+08*	5.7915E-01	1.3016E+00	1.22E+07	3.1267E-01	9.7859E-01
3.75E+08	6.6380E-01	1.3128E+00	1.00E+07	3.3698E-01	9.9039E-01
3.50E+08	7.4080E-01	1.3296E+00	8.19E+06	3.8746E-01	9.7573E-01
3.25E+08	7.6801E-01	1.3394E+00	6.70E+06	1.9931E-01	6.5639E-01
3.00E+08	7.8376E-01	1.3434E+00	5.49E+06	1.4968E-01	5.3713E-01
2.75E+08	8.0047E-01	1.3334E+00	4.49E+06	1.4624E-01	5.6118E-01
2.50E+08	8.0915E-01	1.3254E+00	3.68E+06	1.4599E-01	5.3383E-01
2.25E+08	8.1796E-01	1.3224E+00	3.01E+06	1.2797E-01	5.3862E-01
2.00E+08	7.3489E-01	1.3244E+00	2.46E+06	1.2712E-01	5.4919E-01
1.80E+08	7.7471E-01	1.3194E+00	2.02E+06	1.0315E-01	4.9559E-01
1.60E+08	7.5311E-01	1.3227E+00	1.65E+06	8.3819E-02	3.1461E-01
1.40E+08	8.0410E-01	1.3516E+00	1.35E+06	1.3551E-02	5.1671E-02
1.20E+08	7.8314E-01	1.3583E+00	1.11E+06	1.7806E-03	1.8998E-02
1.10E+08	8.0839E-01	1.4180E+00	9.07E+05	5.9640E-04	6.5292E-03
1.00E+08	8.4285E-01	1.4493E+00	7.43E+05	1.1990E-04	1.0334E-03
9.00E+07	8.6533E-01	1.4845E+00	4.98E+05	1.2951E-05	2.5770E-04
8.00E+07	8.7328E-01	1.5234E+00	3.34E+05	0.0000E+00	9.6159E-05
7.00E+07	8.9851E-01	1.5383E+00	2.24E+05	0.0000E+00	9.9000E-05
6.50E+07	9.0406E-01	1.5893E+00	1.50E+05	0.0000E+00	3.9529E-05
6.00E+07	8.7216E-01	1.6395E+00	8.65E+04	0.0000E+00	6.1295E-05
5.50E+07	7.9173E-01	1.6442E+00	3.18E+04	0.0000E+00	9.6385E-05
5.00E+07	8.2978E-01	1.6656E+00	1.50E+04	0.0000E+00	1.1010E-04
4.50E+07	8.3477E-01	1.6856E+00	7.10E+03	0.0000E+00	6.7200E-06
4.00E+07	7.8467E-01	1.6738E+00	3.35E+03	0.0000E+00	4.0000E-08
3.50E+07	7.5686E-01	1.6621E+00	1.58E+03	0.0000E+00	4.5624E-08
3.00E+07	6.5461E-01	1.6173E+00	4.54E+02	0.0000E+00	8.7118E-08
2.75E+07	6.4635E-01	1.5813E+00	1.01E+02	0.0000E+00	1.8165E-07
2.50E+07	6.4801E-01	1.5717E+00	2.26E+01	0.0000E+00	3.0957E-07
2.25E+07	5.8063E-01	1.4748E+00	1.07E+01	0.0000E+00	4.4716E-07
1.96E+07	5.0863E-01	1.2133E+00	5.04E+00	0.0000E+00	6.4625E-07
1.75E+07	4.4226E-01	1.2344E+00	2.38E+00	0.0000E+00	9.3423E-07
1.49E+07	3.7120E-01	1.1358E+00	1.12E+00	0.0000E+00	1.4397E-06
1.35E+07	3.1923E-01	1.0034E+00	4.14E-01	0.0000E+00	6.3656E-06

* Read as 4.00×10^8

Lowest energy boundary is 1.00E-04 [eV]

Table 9 Calculated response of solid state nuclear track detector.

Energy [MeV]	Response [Pits/n]	Energy [MeV]	Response [Pits/n]
1.00E-01 *	3.64E-04	3.44E+00	9.51E-04
2.00E-01	4.92E-04	3.52E+00	9.24E-04
3.50E-01	5.33E-04	3.80E+00	9.16E-04
4.35E-01	6.59E-04	4.00E+00	9.45E-04
5.00E-01	5.01E-04	4.27E+00	9.52E-04
6.00E-01	5.34E-04	5.00E+00	9.36E-04
8.00E-01	5.52E-04	6.00E+00	9.55E-04
1.00E+00	6.27E-04	6.30E+00	1.02E-03
1.22E+00	6.02E-04	7.00E+00	9.43E-04
1.32E+00	6.95E-04	7.75E+00	9.84E-04
1.65E+00	7.59E-04	8.00E+00	9.44E-04
2.00E+00	7.07E-04	1.00E+01	8.86E-04
2.08E+00	8.29E-04	1.20E+01	7.33E-04
2.35E+00	7.37E-04	1.50E+01	2.85E-04
2.82E+00	8.93E-04	1.60E+01	2.41E-04
2.94E+00	8.66E-04	1.88E+01	2.21E-04
3.00E+00	7.96E-04	2.00E+01	2.16E-04
3.21E+00	8.77E-04		

* Read as 1.00×10^{-1}

Table 10 Neutron spectra behind various thickness polyethylene shield measured with BC501A scintillation counter for 43-MeV p-^{7}Li neutrons.

Upper Energy Boundary	Neutron Flux [n cm^{-2} lethargy^{-1} μC^{-1}], Error [%]							
[eV]	30.5 cm thick		61.0 cm thick		122.0 cm thick		183.0 cm thick	
4.30E+07*	2.18E+04	29.2	2.57E+03	31.0	6.24E+01	32.5	1.11E+00	46.0
4.20E+07	2.64E+04	21.3	3.85E+03	18.5	8.87E+01	20.4	1.90E+00	24.4
4.10E+07	2.73E+04	13.3	4.53E+03	8.8	1.02E+02	9.8	2.48E+00	12.3
4.00E+07	2.44E+04	9.2	4.29E+03	5.4	9.79E+01	5.7	2.61E+00	7.0
3.90E+07	1.92E+04	10.3	3.43E+03	8.5	8.12E+01	8.9	2.41E+00	8.5
3.80E+07	1.35E+04	12.8	2.45E+03	18.5	5.89E+01	19.7	2.07E+00	20.4
3.70E+07	8.67E+03	12.9	1.60E+03	36.5	3.78E+01	39.8	1.63E+00	36.3
3.60E+07	5.46E+03	19.6	9.56E+02	52.7	2.31E+01	56.3	1.12E+00	48.2
3.50E+07	3.78E+03	42.4	5.53E+02	45.6	1.60E+01	40.9	6.95E-01	44.5
3.40E+07	3.12E+03	57.2	3.74E+02	16.0	1.38E+01	11.9	4.51E-01	19.8
3.30E+07	2.96E+03	54.1	3.34E+02	35.6	1.32E+01	23.7	3.50E-01	26.7
3.20E+07	2.97E+03	42.5	3.47E+02	37.5	1.26E+01	27.1	3.16E-01	38.4
3.10E+07	2.98E+03	30.9	3.67E+02	27.7	1.15E+01	23.1	3.02E-01	38.4
3.00E+07	2.97E+03	22.0	3.78E+02	19.6	1.03E+01	18.9	2.88E-01	34.7
2.90E+07	2.92E+03	16.2	3.73E+02	15.5	9.15E+00	16.5	2.71E-01	31.0
2.80E+07	2.85E+03	12.9	3.51E+02	15.3	8.20E+00	17.1	2.53E-01	28.2
2.70E+07	2.76E+03	11.7	3.15E+02	18.5	7.50E+00	20.6	2.36E-01	26.2
2.60E+07	2.66E+03	11.5	2.74E+02	23.6	6.99E+00	24.7	2.21E-01	24.6
2.50E+07	2.54E+03	11.3	2.35E+02	28.3	6.54E+00	27.4	2.10E-01	22.4
2.40E+07	2.40E+03	10.7	2.06E+02	29.3	6.04E+00	27.1	2.03E-01	19.0
2.30E+07	2.25E+03	9.7	1.89E+02	24.5	5.42E+00	23.1	1.99E-01	14.6
2.20E+07	2.09E+03	8.6	1.79E+02	15.7	4.69E+00	16.2	1.98E-01	10.4
2.10E+07	1.91E+03	7.6	1.73E+02	10.5	3.94E+00	12.0	1.96E-01	7.8
2.00E+07	1.74E+03	7.5	1.66E+02	18.2	3.31E+00	23.6	1.92E-01	7.2
1.90E+07	1.57E+03	9.1	1.54E+02	26.8	2.93E+00	36.9	1.83E-01	8.4
1.80E+07	1.42E+03	9.7	1.37E+02	28.3	2.83E+00	36.1	1.71E-01	9.2
1.70E+07	1.28E+03	9.3	1.16E+02	21.5	2.85E+00	23.0	1.58E-01	9.6
1.60E+07	1.15E+03	8.6	9.31E+01	14.3	2.79E+00	13.0	1.46E-01	9.7
1.50E+07	1.03E+03	8.4	7.40E+01	15.8	2.54E+00	12.8	1.36E-01	10.3
1.40E+07	9.02E+02	9.3	6.31E+01	11.6	2.16E+00	9.5	1.28E-01	11.4
1.30E+07	7.64E+02	11.7	5.95E+01	25.8	1.78E+00	23.1	1.21E-01	13.2
1.20E+07	6.25E+02	15.3	5.69E+01	39.3	1.45E+00	41.3	1.12E-01	14.6
1.10E+07	5.01E+02	18.4	5.11E+01	44.0	1.20E+00	50.4	1.02E-01	14.3
1.00E+07	4.09E+02	16.7	4.41E+01	41.5	1.07E+00	45.8	8.85E-02	10.3
9.00E+06	3.58E+02	8.9	3.81E+01	26.2	1.09E+00	24.7	7.34E-02	6.4
8.00E+06	3.36E+02	19.1	3.08E+01	37.8	1.26E+00	25.4	6.20E-02	8.9
7.00E+06	3.20E+02	31.5	2.63E+01	69.2	1.50E+00	45.7	5.88E-02	11.0
6.00E+06	3.01E+02	50.8	3.08E+01	77.6	1.53E+00	15.1	5.98E-02	35.0
5.00E+06	2.67E+02	87.4	2.81E+01	89.1	1.14E+00	88.2	5.41E-02	55.3
4.00E+06								

* Read as 4.30 x 10^{7}

Table 11 Neutron spectra behind 30.5-cm thick polyethylene shield with additional iron collimator measured with BC501A scintillation counter for 43-MeV p-^{7}Li neutrons.

Upper Energy Boundary	Neutron Flux [n cm^{-2} lethargy^{-1} μC^{-1}], Error [%]					
[eV]	beam axis		20 cm from axis		40 cm from axis	
4.30E+07*	1.34E+04	30.9	2.17E+02	16.7	5.90E+00	8.5
4.20E+07	1.90E+04	19.4	3.51E+02	10.0	1.08E+01	6.9
4.10E+07	2.19E+04	10.0	4.74E+02	6.1	1.67E+01	6.0
4.00E+07	2.14E+04	5.2	5.52E+02	5.6	2.27E+01	5.3
3.90E+07	1.86E+04	7.4	5.71E+02	6.2	2.74E+01	4.8
3.80E+07	1.45E+04	16.4	5.35E+02	6.4	2.93E+01	5.5
3.70E+07	9.94E+03	31.3	4.48E+02	5.6	2.76E+01	7.1
3.60E+07	5.87E+03	47.8	3.23E+02	10.5	2.36E+01	7.2
3.50E+07	3.14E+03	52.7	2.08E+02	26.8	1.94E+01	5.4
3.40E+07	1.84E+03	29.3	1.48E+02	35.2	1.68E+01	5.0
3.30E+07	1.48E+03	26.3	1.49E+02	17.0	1.55E+01	6.2
3.20E+07	1.52E+03	33.1	1.75E+02	6.8	1.50E+01	6.9
3.10E+07	1.65E+03	30.3	1.95E+02	11.6	1.48E+01	6.6
3.00E+07	1.76E+03	25.9	2.04E+02	12.2	1.48E+01	5.6
2.90E+07	1.84E+03	22.8	2.05E+02	11.3	1.49E+01	4.9
2.80E+07	1.88E+03	21.1	2.04E+02	10.5	1.50E+01	5.0
2.70E+07	1.88E+03	20.1	2.01E+02	10.4	1.50E+01	6.6
2.60E+07	1.85E+03	19.2	1.97E+02	10.5	1.48E+01	9.6
2.50E+07	1.78E+03	17.7	1.92E+02	10.4	1.46E+01	11.5
2.40E+07	1.70E+03	15.5	1.85E+02	9.6	1.45E+01	10.8
2.30E+07	1.60E+03	12.3	1.77E+02	8.1	1.45E+01	8.5
2.20E+07	1.50E+03	8.8	1.66E+02	6.1	1.45E+01	6.0
2.10E+07	1.40E+03	6.1	1.56E+02	4.6	1.45E+01	4.6
2.00E+07	1.30E+03	5.7	1.47E+02	5.2	1.45E+01	5.4
1.90E+07	1.21E+03	6.9	1.39E+02	6.3	1.45E+01	7.4
1.80E+07	1.11E+03	8.0	1.33E+02	6.2	1.43E+01	7.9
1.70E+07	1.01E+03	8.5	1.29E+02	5.3	1.40E+01	5.6
1.60E+07	9.02E+02	9.1	1.24E+02	4.7	1.33E+01	4.8
1.50E+07	7.87E+02	10.7	1.19E+02	4.5	1.27E+01	5.8
1.40E+07	6.72E+02	14.0	1.12E+02	4.9	1.23E+01	4.6
1.30E+07	5.61E+02	18.9	1.06E+02	6.0	1.21E+01	5.2
1.20E+07	4.61E+02	24.0	9.92E+01	7.2	1.20E+01	6.3
1.10E+07	3.79E+02	25.5	9.28E+01	7.6	1.16E+01	5.9
1.00E+07	3.20E+02	16.9	8.65E+01	6.8	1.09E+01	5.3
9.00E+06	2.84E+02	8.5	8.06E+01	4.6	1.02E+01	4.9
8.00E+06	2.61E+02	30.8	7.54E+01	6.8	9.44E+00	4.5
7.00E+06	2.39E+02	57.6	6.77E+01	7.2	8.54E+00	9.7
6.00E+06	2.07E+02	72.8	5.30E+01	9.5	7.95E+00	4.9
5.00E+06						

* Read as 4.30 x 10^{7}

Table 12 Neutron spectra behind 61.0-cm thick polyethylene shield with additional iron collimator measured with BC501A scintillation counter for 43-MeV p-^{7}Li neutrons.

Upper Energy Boundary [eV]	Neutron Flux [n cm^{-2} lethargy^{-1} μC^{-1}], Error [%]					
	beam axis		20 cm from axis		40 cm from axis	
4.30E+07*	2.42E+03	38.9	1.07E+02	17.4	1.41E+01	6.4
4.20E+07	3.35E+03	24.9	1.76E+02	10.8	1.86E+01	5.6
4.10E+07	3.79E+03	12.7	2.40E+02	7.6	2.28E+01	4.9
4.00E+07	3.64E+03	5.7	2.75E+02	6.9	2.60E+01	4.7
3.90E+07	3.08E+03	9.1	2.74E+02	6.6	2.76E+01	5.1
3.80E+07	2.33E+03	22.8	2.48E+02	6.2	2.76E+01	6.0
3.70E+07	1.56E+03	45.7	2.12E+02	13.3	2.62E+01	6.8
3.60E+07	9.10E+02	71.0	1.69E+02	24.1	2.38E+01	7.1
3.50E+07	4.82E+02	80.2	1.24E+02	29.9	2.12E+01	6.6
3.40E+07	2.70E+02	48.9	8.62E+01	23.7	1.89E+01	5.8
3.30E+07	2.03E+02	41.9	6.32E+01	8.5	1.70E+01	5.7
3.20E+07	2.02E+02	55.7	5.45E+01	14.5	1.56E+01	6.3
3.10E+07	2.19E+02	50.2	5.38E+01	18.5	1.47E+01	6.9
3.00E+07	2.34E+02	41.1	5.56E+01	16.7	1.41E+01	7.4
2.90E+07	2.42E+02	33.7	5.74E+01	14.3	1.36E+01	8.1
2.80E+07	2.43E+02	28.3	5.83E+01	12.7	1.32E+01	9.3
2.70E+07	2.38E+02	24.5	5.81E+01	12.1	1.29E+01	10.7
2.60E+07	2.28E+02	22.0	5.68E+01	11.9	1.25E+01	12.0
2.50E+07	2.13E+02	19.7	5.45E+01	11.5	1.21E+01	12.6
2.40E+07	1.95E+02	17.0	5.13E+01	10.6	1.15E+01	12.1
2.30E+07	1.75E+02	13.8	4.76E+01	9.1	1.08E+01	10.3
2.20E+07	1.56E+02	10.7	4.36E+01	7.2	9.95E+00	7.4
2.10E+07	1.39E+02	9.2	3.97E+01	5.6	9.16E+00	5.0
2.00E+07	1.24E+02	9.6	3.61E+01	5.1	8.47E+00	6.0
1.90E+07	1.10E+02	12.1	3.31E+01	5.7	7.93E+00	7.9
1.80E+07	9.84E+01	14.0	3.05E+01	6.2	7.52E+00	7.9
1.70E+07	8.68E+01	14.9	2.82E+01	6.4	7.17E+00	6.3
1.60E+07	7.51E+01	16.0	2.60E+01	6.7	6.80E+00	5.2
1.50E+07	6.32E+01	18.3	2.37E+01	7.6	6.37E+00	4.9
1.40E+07	5.14E+01	23.1	2.14E+01	9.2	5.89E+00	5.6
1.30E+07	4.07E+01	31.4	1.92E+01	11.5	5.42E+00	7.9
1.20E+07	3.23E+01	41.0	1.72E+01	13.4	4.98E+00	10.4
1.10E+07	2.71E+01	43.3	1.57E+01	12.9	4.57E+00	11.4
1.00E+07	2.60E+01	27.6	1.47E+01	8.2	4.21E+00	9.9
9.00E+06	2.83E+01	13.0	1.43E+01	5.4	3.91E+00	5.0
8.00E+06	3.23E+01	29.1	1.41E+01	12.4	3.67E+00	10.5
7.00E+06	3.52E+01	46.2	1.39E+01	20.3	3.44E+00	16.7
6.00E+06	3.50E+01	74.8	1.36E+01	32.7	3.06E+00	20.9
5.00E+06						

* Read as 4.30 x 10^{7}

Table 13 Neutron spectra behind various thickness polyethylene shield measured with BC501A scintillation counter for 68-MeV p-^{7}Li neutrons.

Upper Energy Boundary [eV]	Neutron Flux [n cm^{-2} lethargy^{-1} μC^{-1}], Error [%]							
	30.5 cm thick		61.0 cm thick		122.0 cm thick		183.0 cm thick	
7.00E+07*	4.66E+04	5.9	1.18E+04	5.9	1.22E+03	5.7	9.59E+01	7.3
6.80E+07	7.13E+04	5.1	1.80E+04	5.1	1.83E+03	5.0	1.37E+02	6.0
6.60E+07	6.43E+04	5.0	1.75E+04	5.0	1.64E+03	5.0	1.19E+02	5.8
6.40E+07	3.43E+04	10.7	1.18E+04	8.9	1.01E+03	10.2	6.60E+01	15.5
6.20E+07	1.39E+04	22.6	6.07E+03	14.3	4.69E+02	18.7	3.00E+01	30.2
6.00E+07	9.62E+03	8.6	2.93E+03	7.8	2.02E+02	11.0	1.87E+01	11.9
5.80E+07	1.05E+04	9.7	2.11E+03	12.3	1.37E+02	16.8	1.68E+01	16.4
5.60E+07	1.13E+04	8.9	2.17E+03	11.7	1.45E+02	16.7	1.62E+01	16.5
5.40E+07	1.17E+04	7.1	2.32E+03	8.7	1.56E+02	12.4	1.52E+01	13.2
5.20E+07	1.18E+04	6.2	2.36E+03	7.3	1.56E+02	9.9	1.39E+01	11.4
5.00E+07	1.16E+04	5.9	2.27E+03	6.9	1.45E+02	9.0	1.23E+01	11.1
4.80E+07	1.10E+04	5.9	2.06E+03	6.9	1.26E+02	8.9	1.06E+01	11.6
4.60E+07	1.00E+04	5.9	1.77E+03	7.3	1.04E+02	9.7	8.92E+00	12.7
4.40E+07	9.19E+03	6.2	1.53E+03	8.0	8.58E+01	11.4	7.77E+00	14.6
4.30E+07	8.60E+03	6.5	1.37E+03	9.0	7.42E+01	13.3	7.08E+00	16.6
4.20E+07	8.02E+03	7.1	1.23E+03	10.3	6.34E+01	16.1	6.46E+00	19.3
4.10E+07	7.48E+03	7.8	1.11E+03	12.1	5.35E+01	20.0	5.89E+00	22.7
4.00E+07	7.00E+03	8.7	1.00E+03	14.0	4.49E+01	25.1	5.36E+00	26.5
3.90E+07	6.58E+03	9.5	9.16E+02	15.9	3.77E+01	31.0	4.86E+00	30.3
3.80E+07	6.21E+03	10.2	8.45E+02	17.4	3.19E+01	37.3	4.38E+00	34.0
3.70E+07	5.89E+03	10.7	7.84E+02	18.6	2.73E+01	43.4	3.92E+00	37.5
3.60E+07	5.60E+03	11.0	7.25E+02	19.5	2.40E+01	48.3	3.49E+00	40.5
3.50E+07	5.33E+03	11.1	6.64E+02	20.3	2.17E+01	51.5	3.13E+00	42.7
3.40E+07	5.06E+03	11.2	6.00E+02	21.1	2.01E+01	52.6	2.86E+00	43.6
3.30E+07	4.79E+03	11.2	5.34E+02	22.0	1.91E+01	51.8	2.69E+00	42.8
3.20E+07	4.52E+03	11.2	4.72E+02	23.0	1.85E+01	49.6	2.62E+00	40.3
3.10E+07	4.25E+03	11.2	4.18E+02	24.0	1.81E+01	47.0	2.62E+00	37.1
3.00E+07	4.00E+03	11.4	3.76E+02	24.8	1.78E+01	44.1	2.63E+00	34.1
2.90E+07	3.77E+03	11.8	3.49E+02	25.3	1.75E+01	41.4	2.61E+00	32.2
2.80E+07	3.55E+03	12.4	3.35E+02	25.4	1.74E+01	38.9	2.52E+00	31.7
2.70E+07	3.34E+03	13.0	3.28E+02	25.1	1.72E+01	36.5	2.37E+00	32.2
2.60E+07	3.13E+03	13.5	3.22E+02	24.6	1.70E+01	34.0	2.18E+00	33.3
2.50E+07	2.91E+03	13.7	3.13E+02	23.6	1.66E+01	31.3	2.01E+00	33.6
2.40E+07	2.67E+03	13.2	2.97E+02	21.9	1.59E+01	28.5	1.89E+00	31.4
2.30E+07	2.42E+03	11.9	2.71E+02	19.5	1.47E+01	25.9	1.84E+00	26.4
2.20E+07	2.14E+03	10.2	2.39E+02	17.0	1.30E+01	24.4	1.84E+00	20.8
2.10E+07	1.86E+03	8.8	2.04E+02	15.5	1.11E+01	25.3	1.84E+00	17.2
2.00E+07	1.59E+03	11.7	1.72E+02	22.7	9.09E+00	31.8	1.80E+00	21.8
1.90E+07	1.35E+03	16.4	1.45E+02	33.0	7.40E+00	46.1	1.70E+00	28.3
1.80E+07	1.15E+03	19.4	1.26E+02	39.4	6.26E+00	56.6	1.55E+00	32.3
1.70E+07	1.01E+03	19.5	1.15E+02	38.6	5.78E+00	57.3	1.39E+00	32.4
1.60E+07	9.10E+02	17.3	1.11E+02	32.2	5.91E+00	48.2	1.27E+00	28.2
1.50E+07	8.44E+02	14.6	1.10E+02	24.7	6.50E+00	35.7	1.23E+00	22.0
1.40E+07	7.84E+02	13.7	1.10E+02	20.4	7.32E+00	26.2	1.22E+00	17.6
1.30E+07	7.15E+02	15.7	1.07E+02	21.3	8.15E+00	22.0	1.22E+00	17.5
1.20E+07	6.36E+02	19.8	1.02E+02	25.3	8.78E+00	21.1	1.19E+00	20.0
1.10E+07	5.59E+02	22.1	9.56E+01	26.6	9.10E+00	19.1	1.18E+00	20.3
1.00E+07	5.03E+02	18.2	9.20E+01	21.0	9.13E+00	14.4	1.19E+00	15.5
9.00E+06	4.73E+02	8.9	9.26E+01	10.9	8.98E+00	10.0	1.24E+00	12.9
8.00E+06	4.57E+02	16.2	9.86E+01	15.9	8.66E+00	10.1	1.28E+00	28.5
7.00E+06	4.18E+02	9.8	1.07E+02	8.9	7.96E+00	13.1	1.21E+00	46.1
6.00E+06	3.29E+02	44.8	1.07E+02	29.0	6.60E+00	39.8	9.71E-01	62.0
5.00E+06								

* Read as 7.00 x 10^{7}

Table 14 Neutron spectra behind 30.5-cm thick polyethylene shield with additional iron collimator measured with BC501A scintillation counter for 68-MeV p-^{7}Li neutrons.

Upper Energy Boundary [eV]	Neutron Flux [n cm^{-2} lethargy^{-1} μC^{-1}], Error [%]					
	beam axis		20 cm from axis		40 cm from axis	
7.00E+07*	3.09E+04	5.9	1.42E+02	6.4	7.41E+00	7.2
6.80E+07	4.79E+04	4.7	2.66E+02	5.7	1.16E+01	5.0
6.60E+07	4.48E+04	7.1	3.22E+02	5.0	1.29E+01	8.3
6.40E+07	2.63E+04	8.7	2.59E+02	8.8	1.13E+01	7.5
6.20E+07	1.20E+04	5.2	1.68E+02	11.2	9.87E+00	4.6
6.00E+07	7.42E+03	12.7	1.28E+02	5.3	9.78E+00	5.6
5.80E+07	7.23E+03	12.0	1.30E+02	6.1	1.03E+01	5.4
5.60E+07	7.64E+03	8.7	1.43E+02	5.6	1.09E+01	4.9
5.40E+07	7.80E+03	7.0	1.55E+02	5.1	1.16E+01	4.8
5.20E+07	7.72E+03	6.5	1.65E+02	4.9	1.24E+01	4.8
5.00E+07	7.49E+03	6.5	1.72E+02	5.0	1.33E+01	4.9
4.80E+07	7.11E+03	6.5	1.77E+02	5.0	1.43E+01	4.9
4.60E+07	6.58E+03	6.5	1.80E+02	4.9	1.52E+01	4.8
4.40E+07	6.08E+03	6.7	1.82E+02	4.8	1.59E+01	4.6
4.30E+07	5.73E+03	7.2	1.84E+02	4.8	1.63E+01	4.6
4.20E+07	5.37E+03	7.8	1.86E+02	4.8	1.68E+01	4.6
4.10E+07	5.05E+03	8.8	1.88E+02	4.9	1.74E+01	4.6
4.00E+07	4.77E+03	9.9	1.91E+02	5.0	1.80E+01	4.7
3.90E+07	4.54E+03	10.7	1.93E+02	5.2	1.87E+01	4.7
3.80E+07	4.37E+03	11.3	1.95E+02	5.2	1.94E+01	4.8
3.70E+07	4.24E+03	11.4	1.97E+02	5.3	2.00E+01	4.9
3.60E+07	4.13E+03	11.2	1.99E+02	5.3	2.06E+01	4.9
3.50E+07	4.03E+03	11.0	1.99E+02	5.4	2.12E+01	5.0
3.40E+07	3.91E+03	10.7	1.98E+02	5.4	2.16E+01	5.1
3.30E+07	3.74E+03	10.5	1.97E+02	5.4	2.18E+01	5.2
3.20E+07	3.54E+03	10.4	1.94E+02	5.4	2.19E+01	5.3
3.10E+07	3.31E+03	10.4	1.90E+02	5.4	2.19E+01	5.4
3.00E+07	3.06E+03	10.5	1.86E+02	5.5	2.18E+01	5.5
2.90E+07	2.83E+03	11.0	1.80E+02	5.7	2.17E+01	5.9
2.80E+07	2.63E+03	11.7	1.74E+02	6.2	2.14E+01	6.4
2.70E+07	2.45E+03	12.7	1.67E+02	6.8	2.11E+01	7.1
2.60E+07	2.28E+03	13.8	1.61E+02	7.4	2.08E+01	7.7
2.50E+07	2.11E+03	14.6	1.54E+02	7.6	2.03E+01	7.9
2.40E+07	1.91E+03	14.5	1.48E+02	7.4	1.98E+01	7.5
2.30E+07	1.70E+03	13.3	1.42E+02	6.5	1.92E+01	6.5
2.20E+07	1.49E+03	10.9	1.36E+02	5.3	1.85E+01	5.2
2.10E+07	1.30E+03	8.3	1.30E+02	4.5	1.78E+01	4.4
2.00E+07	1.14E+03	13.6	1.23E+02	5.0	1.71E+01	4.8
1.90E+07	1.02E+03	19.5	1.16E+02	5.8	1.64E+01	5.5
1.80E+07	9.18E+02	22.2	1.08E+02	5.9	1.58E+01	5.4
1.70E+07	8.24E+02	20.7	1.01E+02	5.4	1.52E+01	4.9
1.60E+07	7.39E+02	16.3	9.51E+01	4.8	1.47E+01	4.5
1.50E+07	6.70E+02	12.0	9.02E+01	4.6	1.43E+01	4.4
1.40E+07	6.11E+02	11.3	8.65E+01	4.7	1.38E+01	4.6
1.30E+07	5.49E+02	15.5	8.32E+01	5.3	1.34E+01	5.1
1.20E+07	4.75E+02	21.7	7.94E+01	6.0	1.29E+01	5.6
1.10E+07	3.95E+02	26.5	7.47E+01	6.2	1.23E+01	5.8
1.00E+07	3.29E+02	25.2	6.94E+01	5.7	1.15E+01	6.0
9.00E+06	2.93E+02	13.4	6.36E+01	4.5	1.04E+01	6.7
8.00E+06	2.86E+02	25.2	5.62E+01	9.1	8.65E+00	8.0
7.00E+06	2.98E+02	20.9	4.52E+01	22.0	6.23E+00	9.9
6.00E+06	2.98E+02	31.1	3.07E+01	38.1		
5.00E+06						

* Read as 7.00 x 10^{7}

Table 15 Neutron spectra behind 61.0-cm thick polyethylene shield with additional iron collimator measured with BC501A scintillation counter for 68-MeV p-^{7}Li neutrons.

Upper Energy Boundary [eV]	Neutron Flux [n cm^{-2} lethargy^{-1} μC^{-1}], Error [%]					
	beam axis		20 cm from axis		40 cm from axis	
7.00E+07*	5.24E+03	10.8	3.87E+02	7.4	1.80E+01	6.4
6.80E+07	1.32E+04	5.1	6.28E+02	5.0	3.10E+01	4.8
6.60E+07	1.64E+04	9.3	6.27E+02	9.0	3.61E+01	6.7
6.40E+07	9.72E+03	10.5	4.37E+02	9.7	2.99E+01	6.4
6.20E+07	3.35E+03	5.2	2.87E+02	4.9	2.25E+01	4.5
6.00E+07	1.73E+03	18.8	2.38E+02	8.6	2.02E+01	5.5
5.80E+07	1.74E+03	17.0	2.31E+02	8.1	2.07E+01	5.3
5.60E+07	1.87E+03	12.7	2.28E+02	6.6	2.17E+01	4.9
5.40E+07	1.93E+03	9.8	2.22E+02	5.9	2.26E+01	4.7
5.20E+07	1.92E+03	7.9	2.14E+02	5.7	2.34E+01	4.7
5.00E+07	1.83E+03	6.9	2.06E+02	5.9	2.41E+01	4.7
4.80E+07	1.68E+03	6.4	1.99E+02	6.0	2.45E+01	4.7
4.60E+07	1.50E+03	6.5	1.90E+02	5.9	2.47E+01	4.7
4.40E+07	1.36E+03	7.1	1.84E+02	5.8	2.47E+01	4.6
4.30E+07	1.26E+03	7.8	1.80E+02	6.0	2.47E+01	4.6
4.20E+07	1.16E+03	8.7	1.77E+02	6.2	2.47E+01	4.6
4.10E+07	1.06E+03	9.9	1.75E+02	6.6	2.47E+01	4.7
4.00E+07	9.74E+02	11.2	1.73E+02	7.1	2.47E+01	4.8
3.90E+07	8.90E+02	12.7	1.72E+02	7.4	2.47E+01	4.9
3.80E+07	8.12E+02	14.1	1.70E+02	7.7	2.46E+01	5.0
3.70E+07	7.42E+02	15.4	1.67E+02	7.8	2.44E+01	5.1
3.60E+07	6.79E+02	16.5	1.64E+02	7.8	2.41E+01	5.1
3.50E+07	6.23E+02	17.4	1.58E+02	7.7	2.36E+01	5.2
3.40E+07	5.74E+02	17.9	1.51E+02	7.7	2.30E+01	5.3
3.30E+07	5.31E+02	18.2	1.43E+02	7.7	2.23E+01	5.4
3.20E+07	4.92E+02	18.2	1.35E+02	7.7	2.15E+01	5.5
3.10E+07	4.56E+02	18.0	1.26E+02	7.7	2.06E+01	5.6
3.00E+07	4.23E+02	17.9	1.18E+02	7.9	1.97E+01	5.8
2.90E+07	3.91E+02	17.7	1.10E+02	8.2	1.88E+01	6.2
2.80E+07	3.59E+02	17.8	1.03E+02	8.8	1.78E+01	6.9
2.70E+07	3.26E+02	17.9	9.63E+01	9.7	1.69E+01	7.9
2.60E+07	2.94E+02	18.1	9.06E+01	10.5	1.60E+01	8.8
2.50E+07	2.63E+02	18.1	8.52E+01	11.0	1.51E+01	9.4
2.40E+07	2.33E+02	17.8	7.98E+01	10.8	1.43E+01	9.1
2.30E+07	2.07E+02	17.3	7.43E+01	9.5	1.35E+01	7.9
2.20E+07	1.85E+02	16.9	6.85E+01	7.5	1.27E+01	6.0
2.10E+07	1.66E+02	17.1	6.27E+01	5.7	1.19E+01	4.6
2.00E+07	1.50E+02	18.2	5.68E+01	8.2	1.11E+01	5.5
1.90E+07	1.36E+02	22.9	5.12E+01	11.2	1.04E+01	6.8
1.80E+07	1.22E+02	26.3	4.61E+01	12.5	9.64E+00	6.9
1.70E+07	1.07E+02	28.2	4.18E+01	11.3	8.96E+00	6.0
1.60E+07	9.13E+01	29.0	3.87E+01	8.7	8.39E+00	5.0
1.50E+07	7.53E+01	29.3	3.66E+01	6.8	7.95E+00	4.7
1.40E+07	6.03E+01	30.5	3.51E+01	6.7	7.63E+00	5.0
1.30E+07	4.82E+01	34.4	3.38E+01	8.3	7.33E+00	6.2
1.20E+07	4.06E+01	39.9	3.22E+01	10.1	6.97E+00	7.4
1.10E+07	3.84E+01	38.2	3.03E+01	10.8	6.54E+00	7.7
1.00E+07	4.10E+01	26.4	2.86E+01	9.4	6.06E+00	6.9
9.00E+06	4.64E+01	15.7	2.73E+01	5.7	5.55E+00	4.6
8.00E+06	5.15E+01	11.7	2.61E+01	9.0	5.05E+00	7.1
7.00E+06	5.26E+01	22.4	2.36E+01	8.9	4.62E+00	7.4
6.00E+06	4.71E+01	53.1	1.88E+01	14.6	4.10E+00	9.3
5.00E+06						

* Read as 7.00 x 10^{7}

Table 16 Counting rates behind the polyethylene shields measured with Bonner ball counter for 43 MeV p-^{7}Li neutrons.

Moderator Thickness	Count Rate [counts μC^{-1}] Error[%]							
	30.5 cm thick[a]		61.0 cm thick		122.0 cm thick		183.0 cm thick	
Bare	3.69E+03[b]	5.27	5.22E+02	5.13	1.73E+01	5.10	1.07E+00	5.45
1.5 cm	3.17E+03	5.18	4.22E+02	5.10	1.46E+01	5.10	8.96E-01	5.47
3.0 cm	4.37E+03	5.27	5.88E+02	5.11	2.04E+01	5.10	1.15E+00	5.37
5.0 cm	6.74E+03	5.15	9.46E+02	5.12	2.99E+01	5.09	1.59E+00	5.36
9.0 cm	7.78E+03	5.18	1.19E+03	5.14	3.86E+01	5.09	1.86E+00	5.24

a Polyethylene shield thickness
b Read as 3.69 x 10^{3}

Table 17 Counting rates behind the polyethylene shields measured with Bonner ball counter for 68 MeV p-^{7}Li neutrons.

Moderator Thickness	Count Rate [counts μC^{-1}] Error[%]							
	30.5 cm thick[a]		61.0 cm thick		122.0 cm thick		183.0 cm thick	
Bare	7.01E+03[b]	5.17	1.49E+03	5.09	1.28E+02	5.09	1.73E+01	5.07
1.5 cm	6.09E+03	5.13	1.36E+03	5.11	1.13E+02	5.10	1.30E+01	5.10
3.0 cm	8.75E+03	5.20	1.75E+03	5.09	1.56E+02	5.10	2.01E+01	5.09
5.0 cm	1.34E+04	5.25	2.96E+03	5.09	2.42E+02	5.09	2.92E+01	5.08
9.0 cm	1.61E+04	5.32	3.76E+03	5.11	3.38E+02	5.10	3.75E+01	5.08

a Polyethylene shield thickness
b Read as 7.01 x 10^{3}

Table 18 Neutron spectra behind the polyethylene shields measured with Bonner ball counter for 43-MeV p-^{7}Li neutrons.

Upper Energy Boundary [eV]	Neutron Flux [n cm^{-2} lethargy^{-1} μC^{-1}]			
	30.5cm thick [a]	61.0cm thick	122.0cm thick	183.0cm thick
4.50E+07 [b]	6.45E+03	1.20E+03	3.24E+01	1.14E+00
3.50E+07	1.23E+03	2.09E+02	6.44E+00	2.89E-01
2.75E+07	1.06E+03	1.28E+02	3.29E+00	2.12E-01
2.25E+07	6.85E+02	7.22E+01	1.93E+00	8.06E-02
1.75E+07	4.60E+02	4.42E+01	1.48E+00	7.32E-02
1.35E+07	3.09E+02	3.20E+01	1.34E+00	1.01E-01
1.00E+07	1.96E+02	2.57E+01	1.01E+00	6.22E-02
6.70E+06	1.33E+02	2.21E+01	8.66E-01	4.49E-02
4.49E+06	1.10E+02	1.67E+01	7.31E-01	3.30E-02
3.01E+06	9.87E+01	1.59E+01	5.85E-01	2.52E-02
2.02E+06	9.30E+01	1.38E+01	4.79E-01	2.75E-02
1.35E+06	7.46E+01	1.26E+01	3.52E-01	2.50E-02
9.07E+05	6.71E+01	8.93E+00	2.74E-01	1.56E-02
4.98E+05	4.83E+01	6.81E+00	2.62E-01	1.14E-02
2.24E+05	3.38E+01	4.71E+00	1.67E-01	1.04E-02
8.65E+04	2.72E+01	3.27E+00	1.29E-01	8.75E-03
1.50E+04	1.97E+01	2.49E+00	7.13E-02	6.35E-03
3.35E+03	2.04E+01	2.32E+00	7.85E-02	4.01E-03
4.54E+02	2.14E+01	2.39E+00	9.81E-02	5.91E-03
2.26E+01	1.72E+01	2.28E+00	7.20E-02	5.34E-03
5.04E+00	1.60E+01	2.04E+00	6.34E-02	1.67E-03
1.12E+00	1.22E+01	1.90E+00	5.45E-02	4.97E-03
4.14E-01	1.92E+01	2.77E+00	9.31E-02	5.74E-03
1.00E-04				

a Polyethylene shield thickness
b Read as 4.50 x 10^{7}

Table 19 Neutron spectra behind the polyethylene shields measured with Bonner ball counter for 68-MeV p-^{7}Li neutrons.

Upper Energy Boundary [eV]	Neutron Flux [n cm^{-2} lethargy^{-1} μC^{-1}]			
	30.5cm thick [a]	61.0cm thick	122.0cm thick	183.0cm thick
8.00E+07[b]	5.17E+03	1.63E+03	1.62E+02	1.60E+01
6.50E+07	1.76E+04	5.00E+03	4.35E+02	3.89E+01
5.50E+07	4.54E+03	1.09E+03	7.84E+01	8.18E+00
4.50E+07	3.40E+03	6.67E+02	3.90E+01	4.47E+00
3.50E+07	2.25E+03	3.54E+02	2.14E+01	2.37E+00
2.75E+07	1.31E+03	1.86E+02	1.24E+01	1.83E+00
2.25E+07	6.97E+02	1.02E+02	9.76E+00	1.36E+00
1.75E+07	4.32E+02	7.40E+01	7.12E+00	7.78E-01
1.35E+07	3.16E+02	6.01E+01	6.51E+00	9.62E-01
1.00E+07	2.30E+02	4.88E+01	5.61E+00	6.30E-01
6.70E+06	1.94E+02	4.62E+01	5.03E+00	7.52E-01
4.49E+06	1.76E+02	4.50E+01	4.81E+00	7.39E-01
3.01E+06	1.81E+02	4.11E+01	4.28E+00	7.06E-01
2.02E+06	1.69E+02	3.81E+01	3.48E+00	4.81E-01
1.35E+06	1.59E+02	3.04E+01	2.88E+00	3.50E-01
9.07E+05	1.34E+02	2.48E+01	2.27E+00	3.65E-01
4.98E+05	9.52E+01	1.97E+01	1.70E+00	2.05E-01
2.24E+05	6.94E+01	1.24E+01	1.21E+00	1.47E-01
8.65E+04	5.28E+01	1.13E+01	8.16E-01	8.66E-02
1.50E+04	4.38E+01	9.50E+00	6.81E-01	7.42E-02
3.35E+03	4.52E+01	8.04E+00	6.26E-01	9.35E-02
4.54E+02	4.09E+01	8.76E+00	7.95E-01	8.12E-02
2.26E+01	3.01E+01	6.28E+00	5.73E-01	6.48E-02
5.04E+00	2.90E+01	6.91E+00	4.80E-01	6.72E-02
1.12E+00	2.32E+01	5.31E+00	4.42E-01	2.71E-02
4.14E-01	3.65E+01	7.79E+00	6.80E-01	9.48E-02
1.00E-04				

a Polyethylene shield thickness
b Read as 8.00 x 10^{7}

Table 20 Fission rates of ^{238}U and ^{232}Th fission counter measured behind the polyethylene shield.

Ep [MeV]	Shield Thickness [cm]	^{238}U Fission Rate [barn cm^{-2} μC^{-1}]	^{238}U Error [%]	^{232}Th Fission Rate [barn cm^{-2} μC^{-1}]	^{232}Th Error [%]
43	0.0	7.28E+04 [a]	0.4	3.07E+04	0.6
	30.5	8.14E+03	5.0	4.29E+03	5.1
	61.0	9.64E+02	5.4	-	-
	122.0	2.42E+01	11.7	2.45E+01	8.9
68	0.0	1.18E+05	0.4	5.71E+04	0.5
	30.5	4.04E+04	5.1	2.85E+04	5.3
	61.0	8.74E+03	5.3	5.51E+03	5.5
	122.0	3.91E+02	5.4	2.12E+02	5.9

a Read as 7.28 x 10^4

Table 21 Reaction rate of solid state nuclear track detector measured inside the 183.0-cm thick polyethylene shield.

Depth[a] [cm]	43 MeV Reaction Rate [Pits cm^{-2} μC^{-1}]	43 MeV Error [%]	68 MeV Reaction Rate [Pits cm^{-2} μC^{-1}]	68 MeV Error [%]
0.0	1.60E+01[b]	6.5	2.77E+01	5.9
30.5	1.26E+00	11.67	3.26E+00	8.2
61.0	1.60E-01	13.13	6.31E-01	9.0
91.5	1.60E-02	31.25	1.51E-01	13.25
122.0	UD[c]		4.80E-02	20.83

a Depth of the polyethylene shield where detectors were placed
b Read as 1.60 x 10^1
c under detection limit

Table 22 Neutron dose-equivalent behind the polyethylene shields measured with the rem counter (Fuji Co. Ltd.).

Shield Thickness [cm]	43 MeV Dose Equivalent [μSv μC^{-1}]	43 MeV Error [%]	68 MeV Dose Equivalent [μSv μC^{-1}]	68 MeV Error [%]
0.0	4.23E+00*	0.52	4.58E+00	0.45
30.5	3.15E-01	1.56	9.35E-01	1.39
61.0	4.37E-02	1.21	2.35E-01	1.23
122.0	1.21E-03	2.48	1.11E-02	1.53
183.0	6.16E-05	10.23	1.76E-03	2.22

* Read as 4.23 x 10^{0}

Table 23 Neutron dose-equivalent behind the polyethylene shields estimated from the measured neutron spectra of BC501A scintillation counter (>10 MeV) and Bonner ball counter (<10 MeV).

Shield Thickness [cm]	43 MeV Dose Equivalent [μSv μC^{-1}]	43 MeV Error [%]	68 MeV Dose Equivalent [μSv μC^{-1}]	68 MeV Error [%]
0.0	2.33E+01*	-	3.53E+01	-
30.5	2.75E+00	25.9	6.92E+00	26.6
61.0	3.88E-01	28.9	1.54E+00	31.4
122.0	9.76E-03	27.6	1.26E-01	36.2
183.0	3.25E-04	24.8	1.06E-02	32.8

* Read as 2.33 x 10^{1}

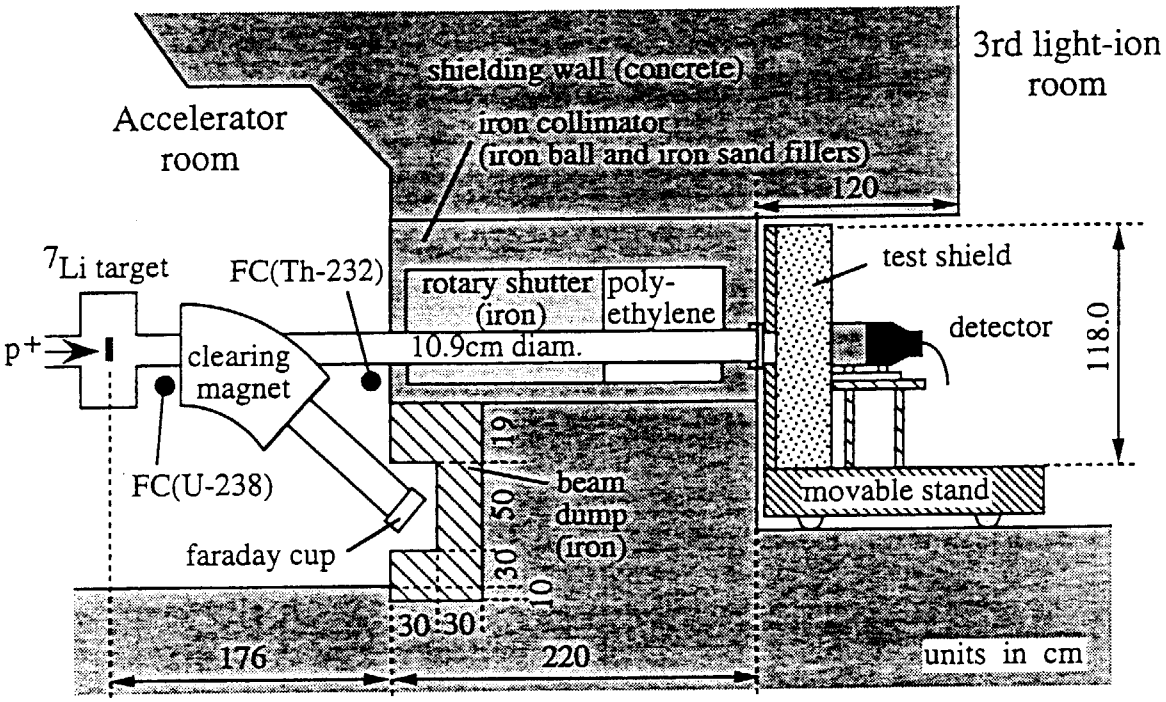

Fig.1 Cross sectional view of the TIARA neutron facility with the experimental arrangement.

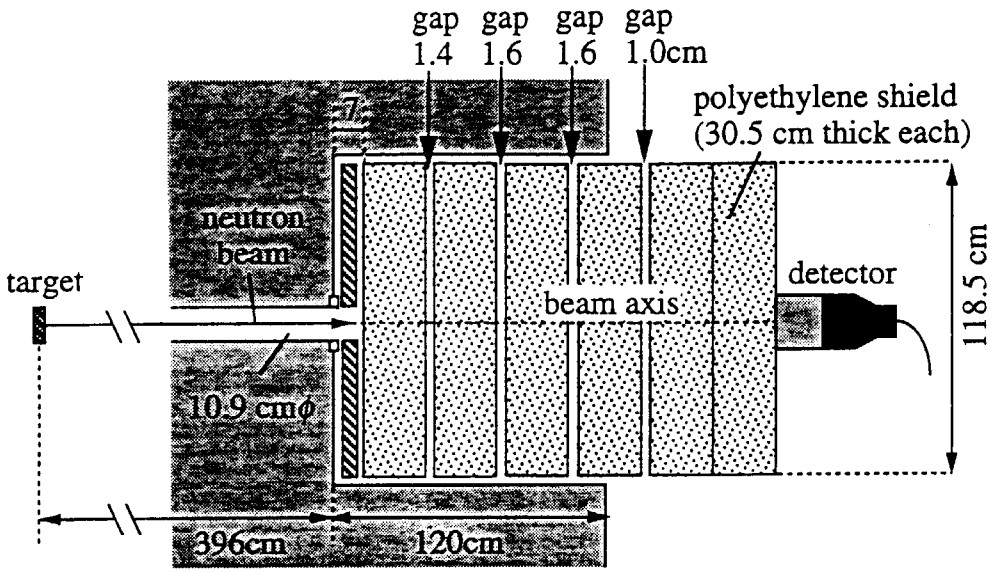

(a)

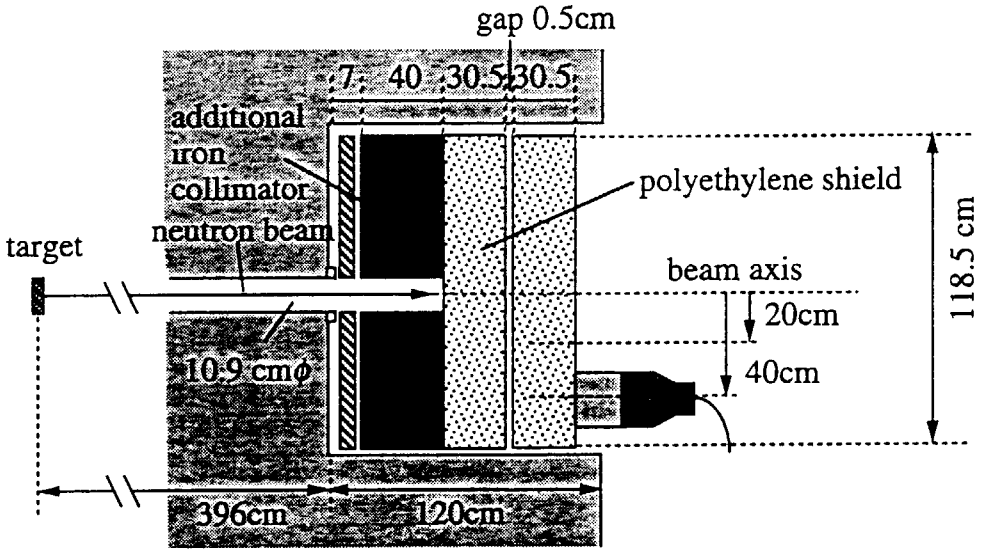

(b)

Fig. 2. Experimental arrangement of shield assembly and detector (a) on measurement on the beam axis and (b) on measurement at distance off the beam axis using additional iron collimator (43 MeV : 40cm thick, 68 MeV: 80 cm thick)

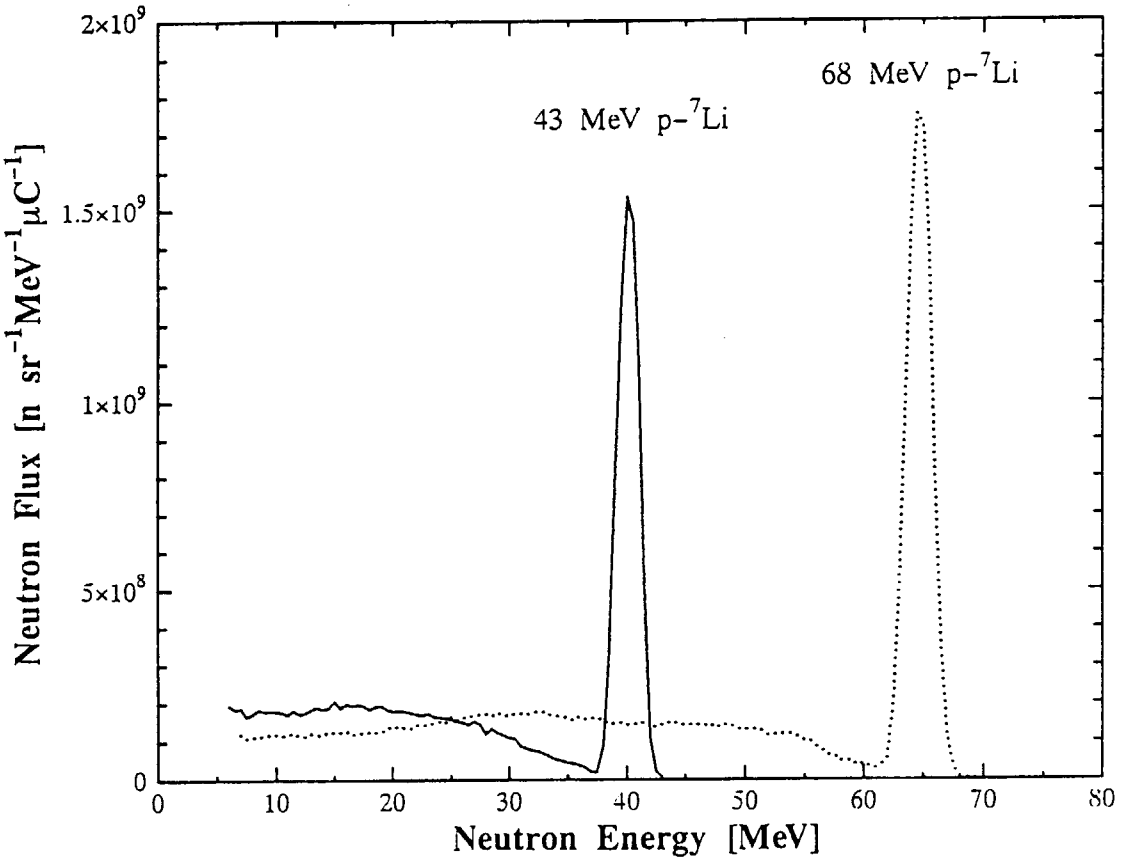

Fig.3 Energy spectra of source neutrons generated by ^{7}Li(p,n) reaction using 43- and 68-MeV protons. These spectra were obtained by TOF measurements and the absolute peak fluxes were given by PRT measurements. The low energy limit of the spectra obtained by the TOF measuremnts are 7 MeV.

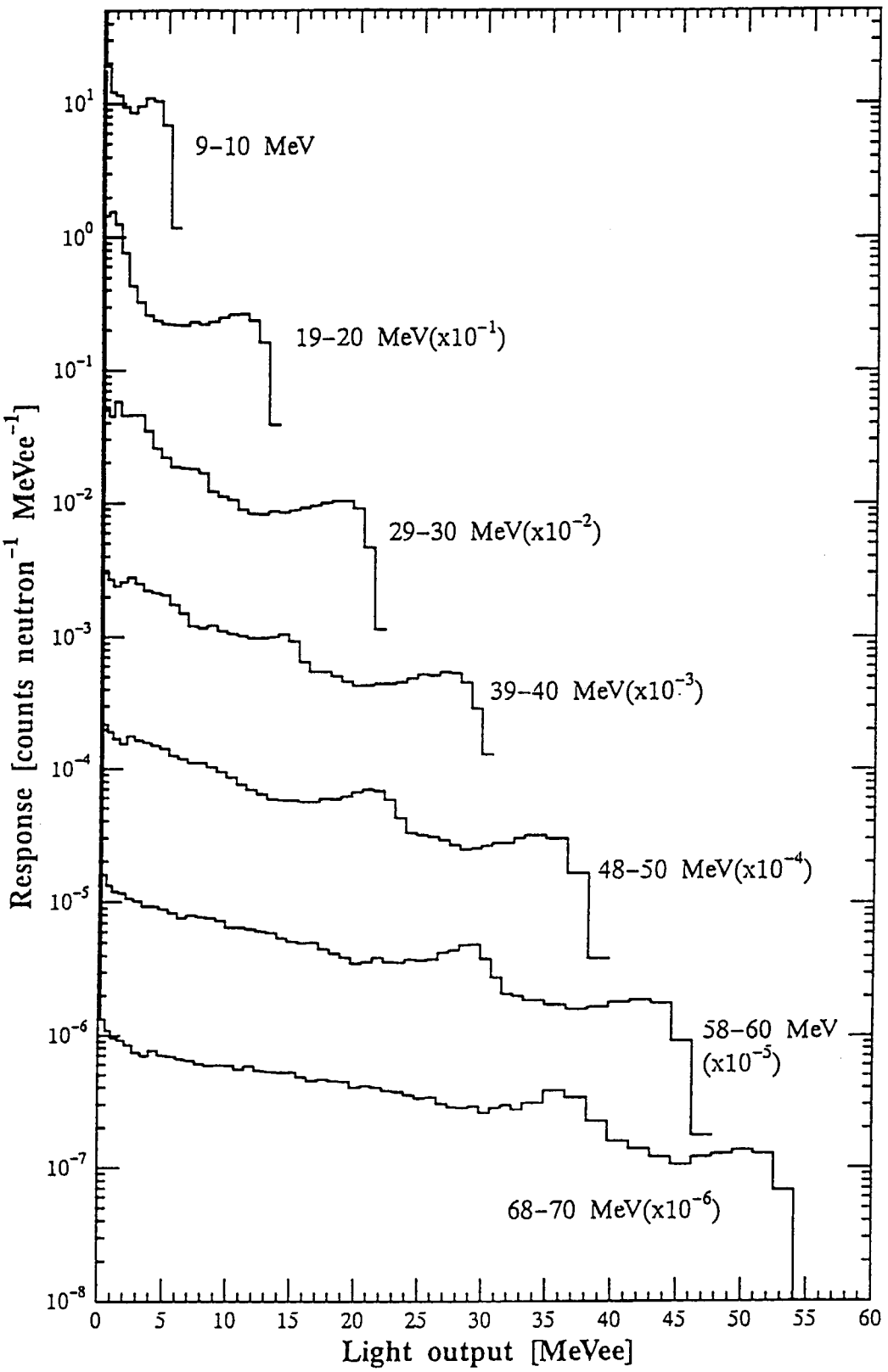

Fig.4 Responses of BC501A scintillation counter to neutrons.

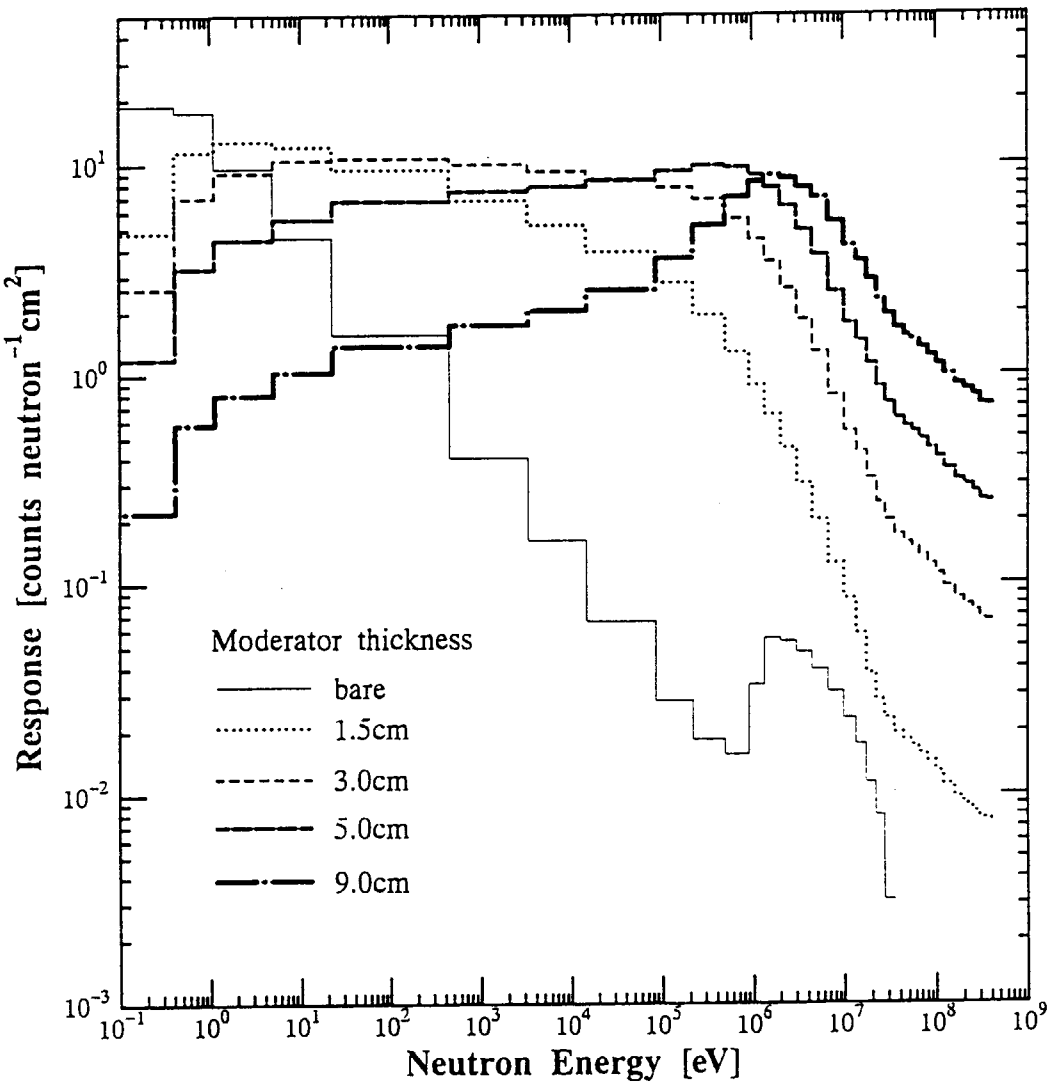

Fig.5 Responses of the Bonner ball counter to neutrons for each moderator thickness.

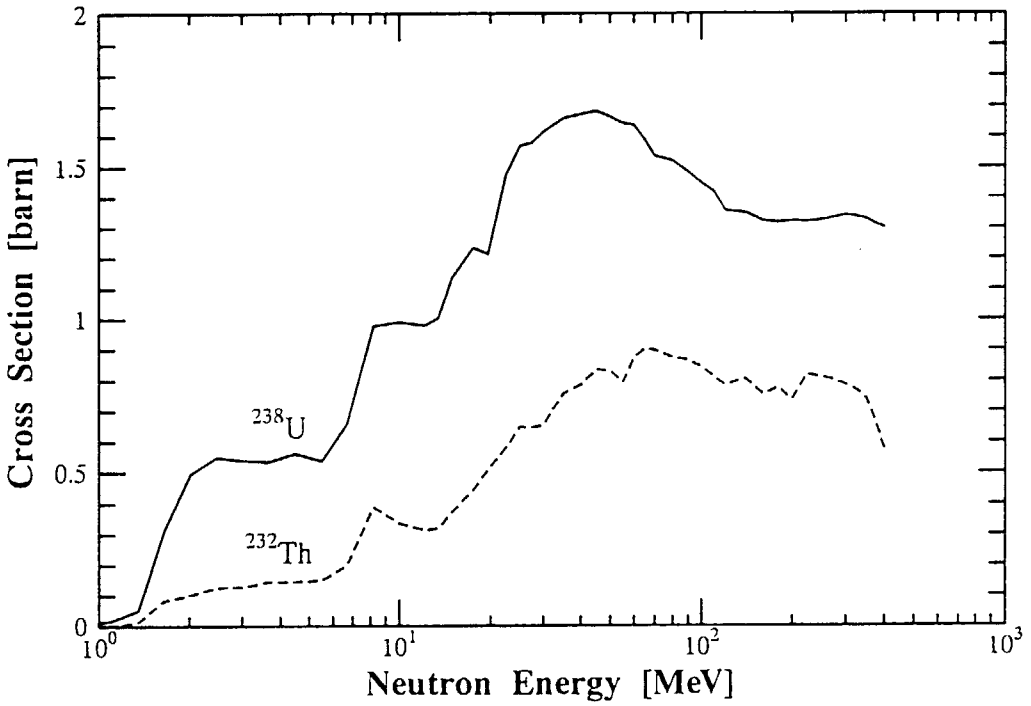

Fig.6 Fission cross sections of ^{238}U and ^{232}Th. The cross sections up to 20 MeV is taken from JENDL-3, and those between 20 to 400 MeV are quoted from the data measured by Lisowski et al.

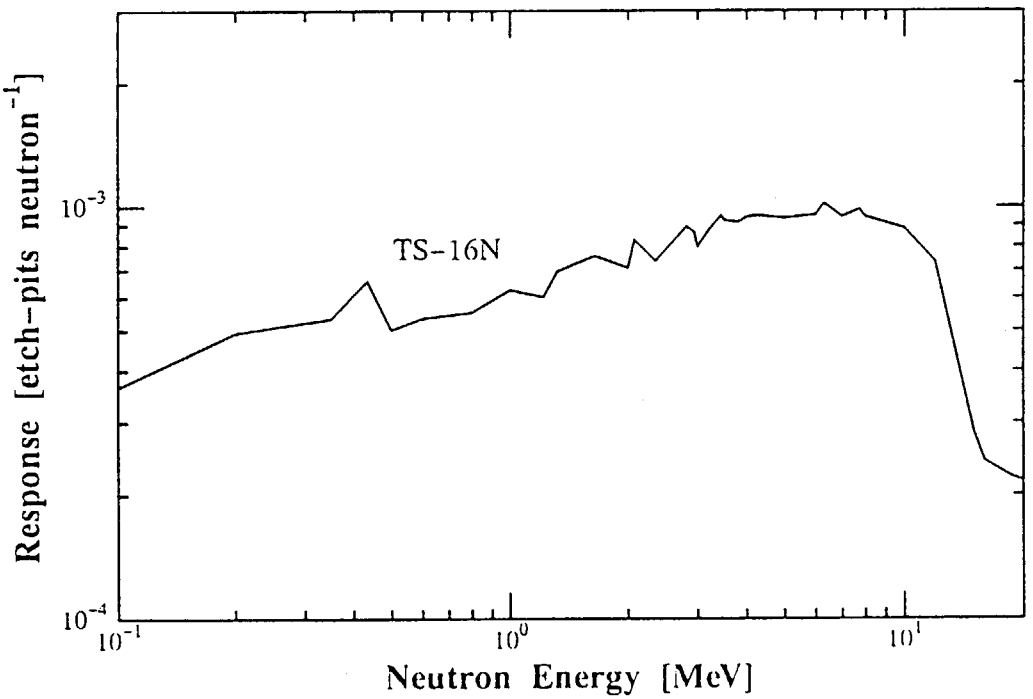

Fig.7 Calculated response of SSNTD to neutrons.

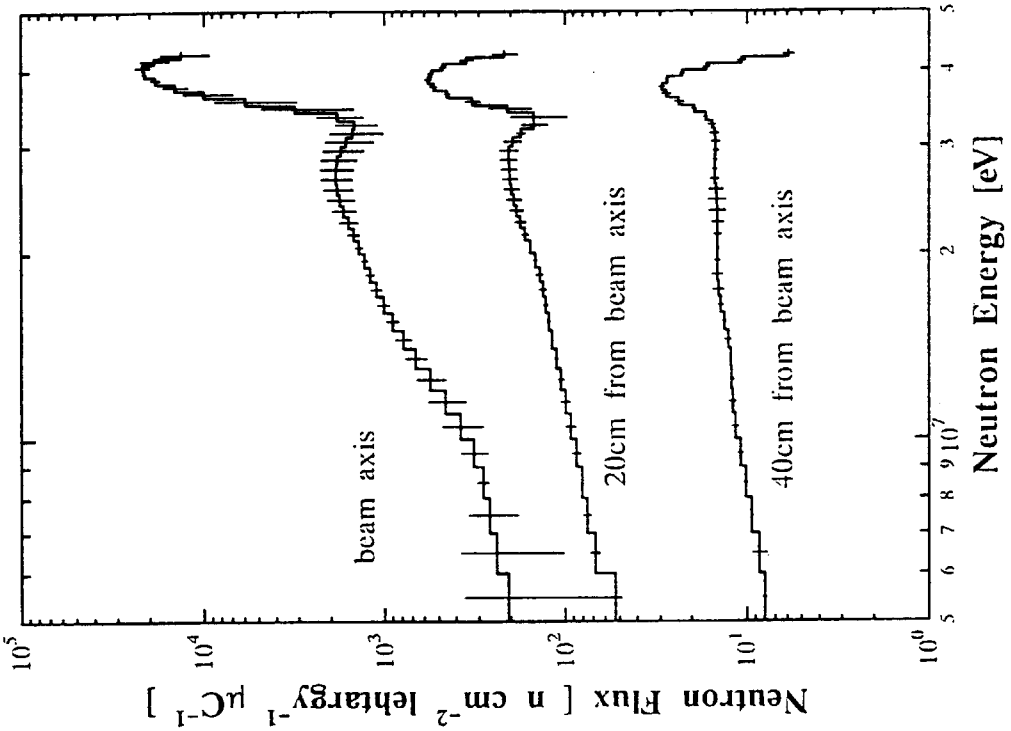

Fig.9 Neutron spectra behind 30.5-cm thick polyethylene shield measured with BC501A scintillation counter for 43 MeV p-^{7}Li neutrons.

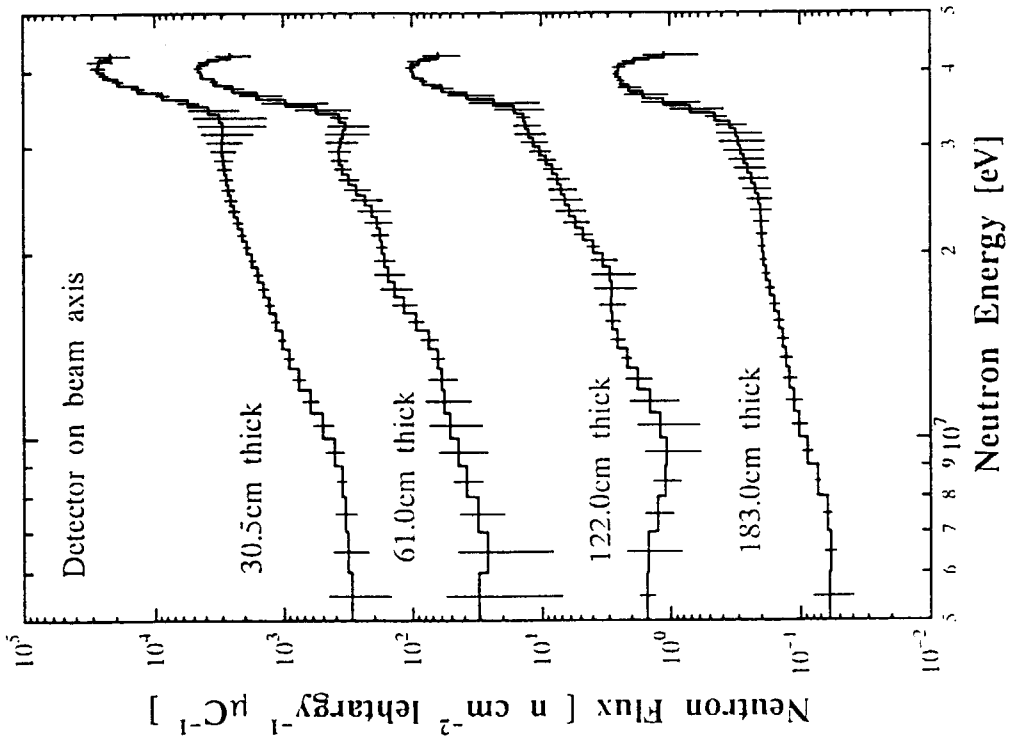

Fig.8 Neutron spectra behind various thickness polyethylene shields measured with BC501A scintillation counter on the beam axis for 43 MeV p-^{7}Li neutrons.

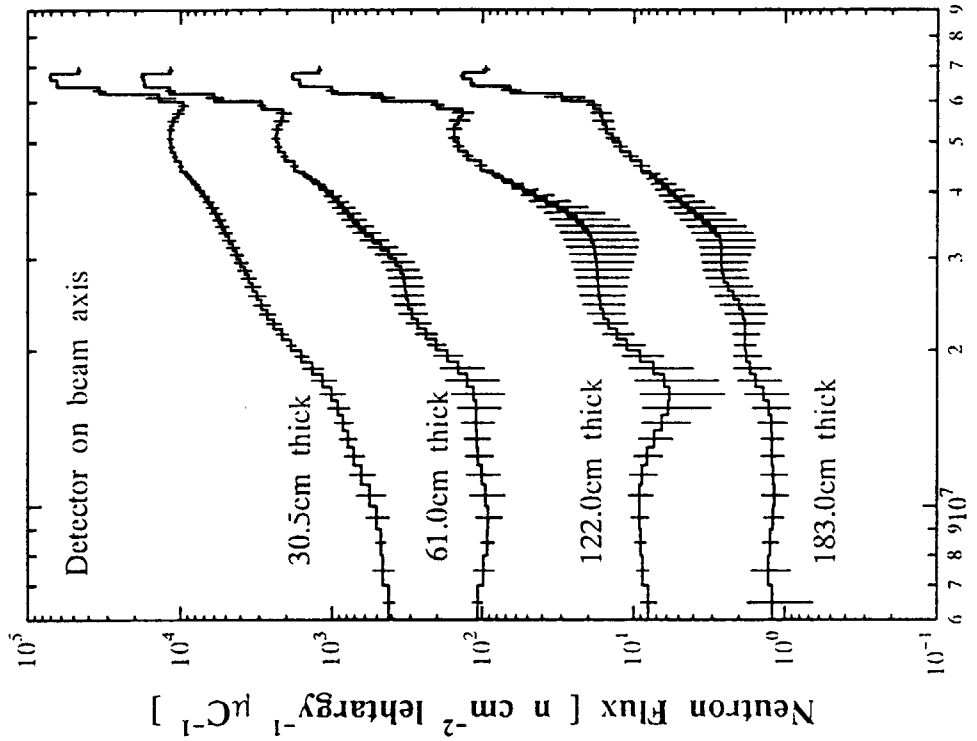

Fig.11 Neutron spectra behind various thickness polyethylene shields measured with BC501A scintillation counter on the beam axis for 68 MeV p-^{7}Li neutrons.

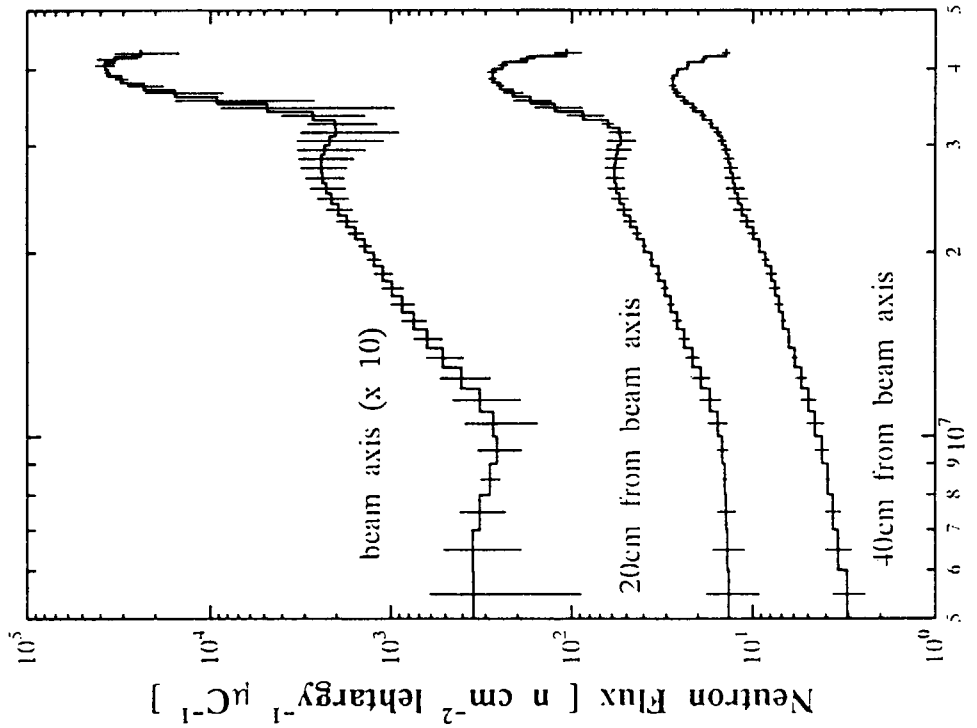

Fig.10 Neutron spectra behind 61.0-cm thick polyethylene shield measured with BC501A scintillation counter for 43 MeV p-^{7}Li neutrons.

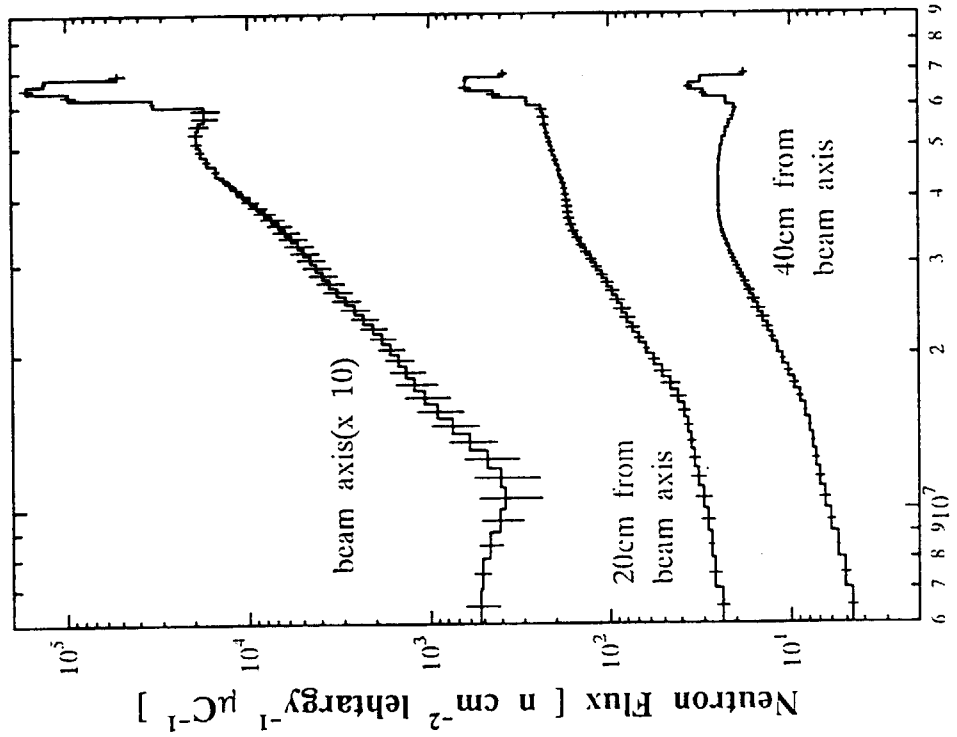

Fig.13 Neutron spectra behind 61.0-cm thick polyethylene shield measured with BC501A scintillation counter for 68 MeV p-^{7}Li neutrons.

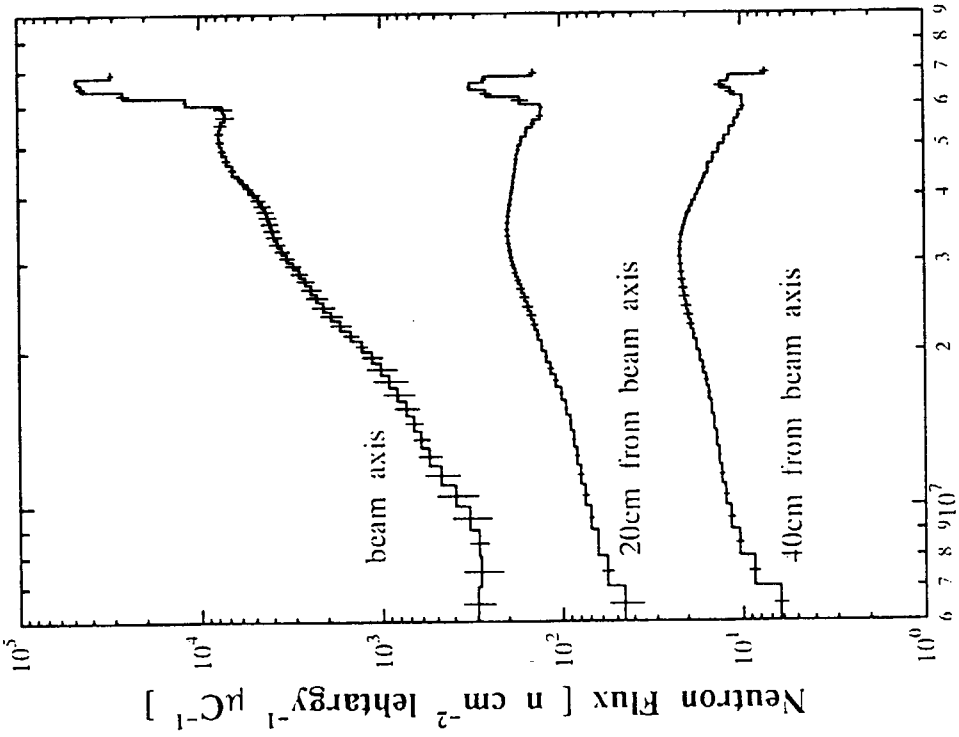

Fig.12 Neutron spectra behind 30.5-cm thick polyethylene shield measured with BC501A scintillation counter for 68 MeV p-^{7}Li neutrons.

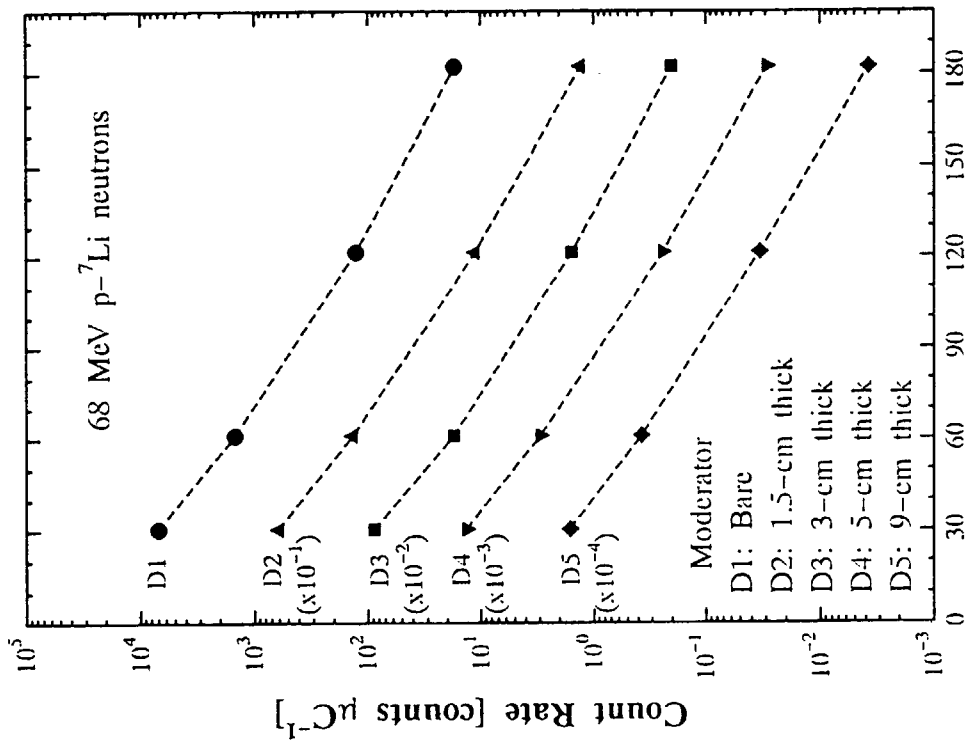

Fig.15 Measured count rates of ^{3}He counter with four kinds of moderators and a bare counter behind polyethylene shield for 68 MeV p-^{7}Li neutrons.

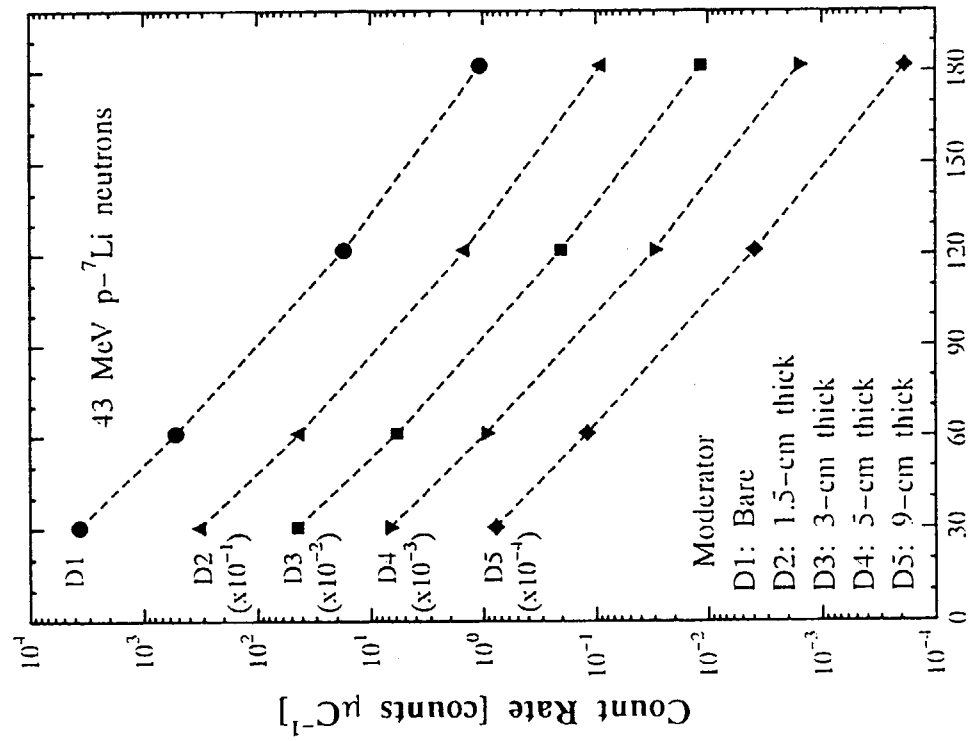

Fig.14 Measured count rates of ^{3}He counter with four kinds of moderators and a bare counter behind polyethylene shield for 43 MeV p-^{7}Li neutrons.

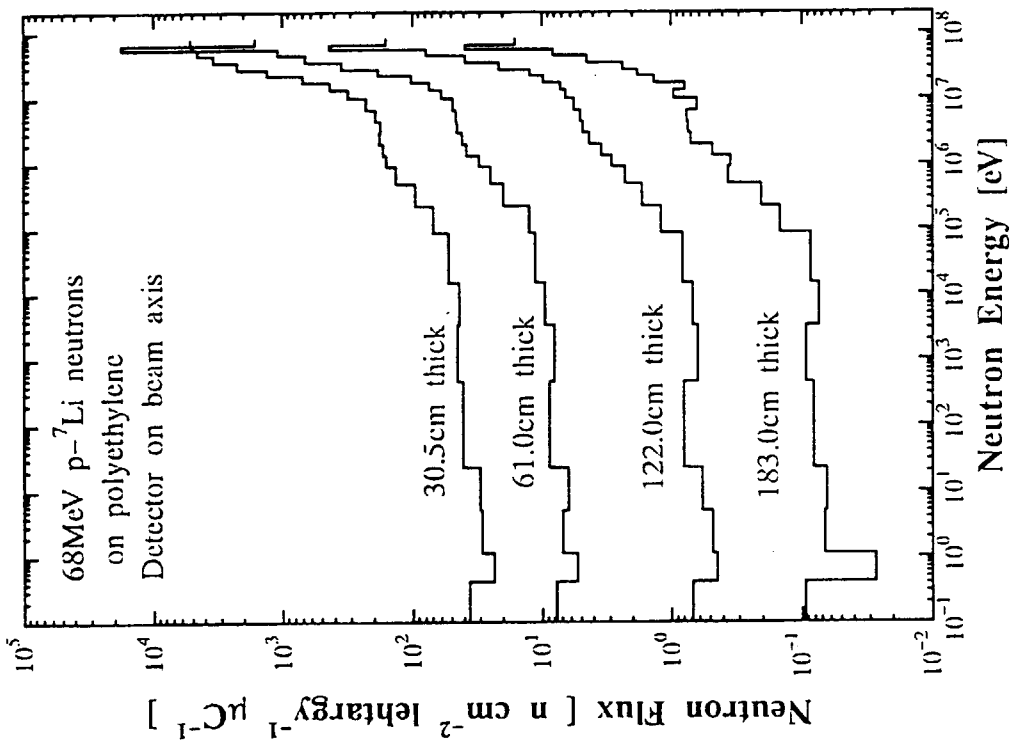

Fig.17 Neutron spectra behind various thickness polyethylene shields measured with Bonner ball counter for 68 MeV p-^{7}Li neutrons.

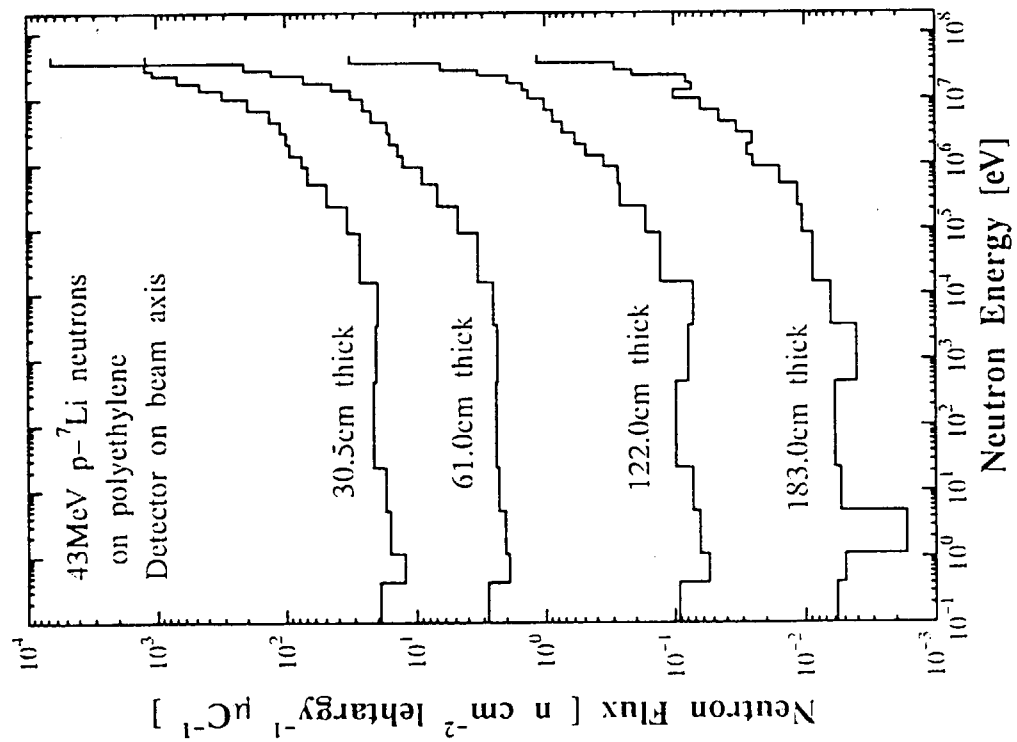

Fig.16 Neutron spectra behind various thickness polyethylene shields measured with Bonner ball counter for 43 MeV p-^{7}Li neutrons.

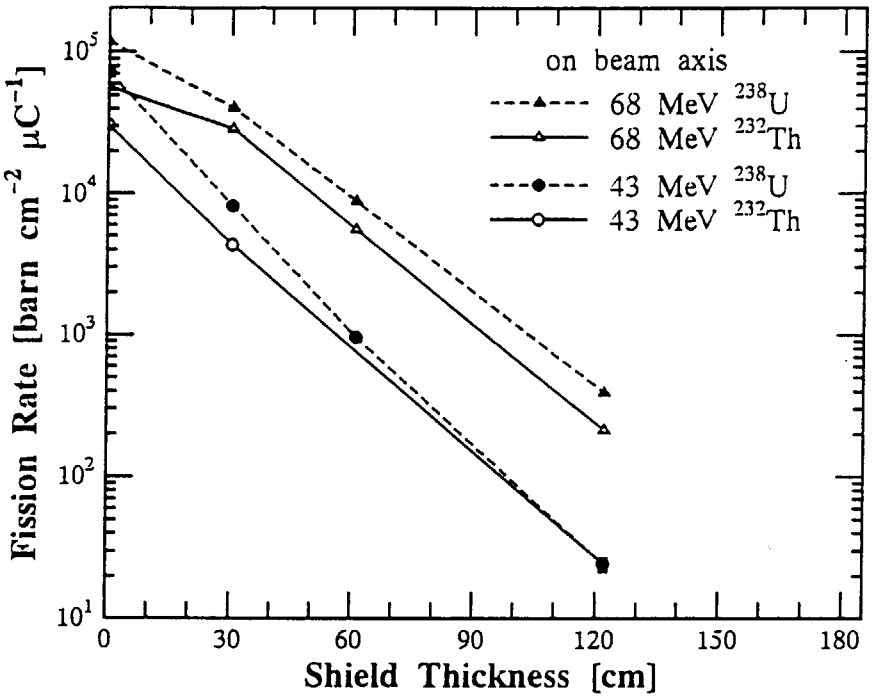

Fig.18 Measured fission rates of ^{238}U and ^{232}Th behind polyethylene shield.

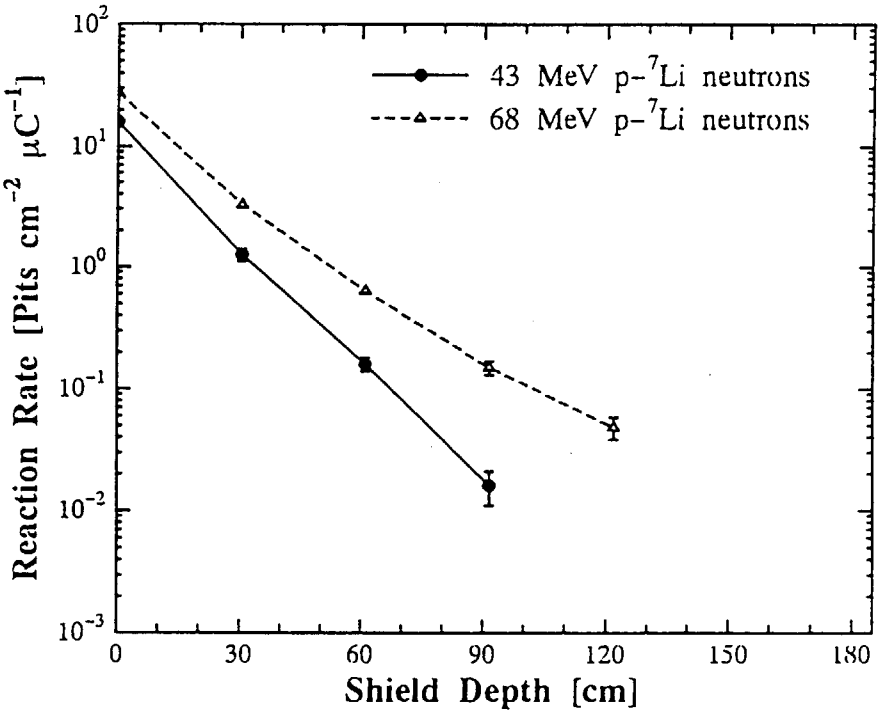

Fig.19 Measured reaction rates of SSNTD inside 183.0-cm thick polyethylene shield.

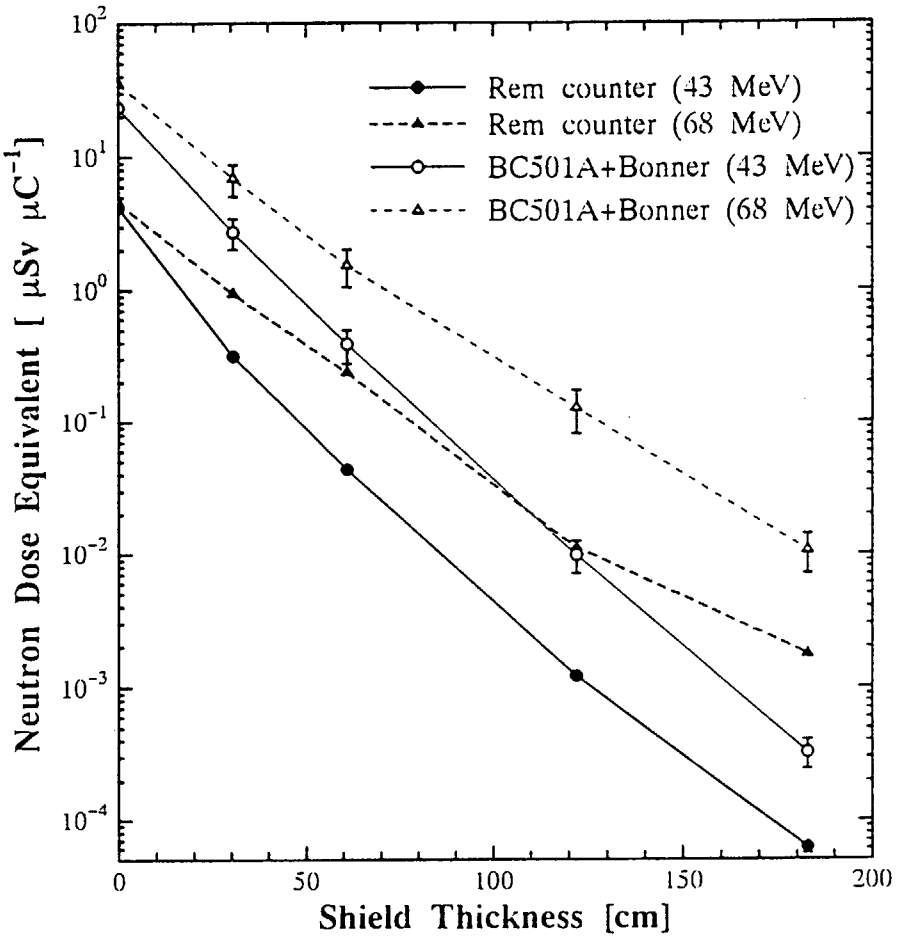

Fig.20 Neutron dose equivalent measured with the rem counter for 43- and 68-MeV p-^{7}Li neutrons. Neutron dose equivalent estimated from neutron spectra measured with BC501A scintillation counter and Bonner ball counter are also shown.

国際単位系（SI）と換算表

表1　SI基本単位および補助単位

量	名称	記号
長さ	メートル	m
質量	キログラム	kg
時間	秒	s
電流	アンペア	A
熱力学温度	ケルビン	K
物質量	モル	mol
光度	カンデラ	cd
平面角	ラジアン	rad
立体角	ステラジアン	sr

表2　SIと併用される単位

名称	記号
分，時，日	min, h, d
度，分，秒	°, ′, ″
リットル	l, L
トン	t
電子ボルト	eV
原子質量単位	u

1 eV=1.60218×10^{-19}J

1 u=1.66054×10^{-27}kg

表5　SI接頭語

倍数	接頭語	記号
10^{18}	エクサ	E
10^{15}	ペタ	P
10^{12}	テラ	T
10^{9}	ギガ	G
10^{6}	メガ	M
10^{3}	キロ	k
10^{2}	ヘクト	h
10^{1}	デカ	da
10^{-1}	デシ	d
10^{-2}	センチ	c
10^{-3}	ミリ	m
10^{-6}	マイクロ	μ
10^{-9}	ナノ	n
10^{-12}	ピコ	p
10^{-15}	フェムト	f
10^{-18}	アト	a

表3　固有の名称をもつSI組立単位

量	名称	記号	他のSI単位による表現
周波数	ヘルツ	Hz	s^{-1}
力	ニュートン	N	m·kg/s^2
圧力，応力	パスカル	Pa	N/m^2
エネルギー，仕事，熱量	ジュール	J	N·m
工率，放射束	ワット	W	J/s
電気量，電荷	クーロン	C	A·s
電位，電圧，起電力	ボルト	V	W/A
静電容量	ファラド	F	C/V
電気抵抗	オーム	Ω	V/A
コンダクタンス	ジーメンス	S	A/V
磁束	ウェーバ	Wb	V·s
磁束密度	テスラ	T	Wb/m^2
インダクタンス	ヘンリー	H	Wb/A
セルシウス温度	セルシウス度	℃	
光束	ルーメン	lm	cd·sr
照度	ルクス	lx	lm/m^2
放射能	ベクレル	Bq	s^{-1}
吸収線量	グレイ	Gy	J/kg
線量等量	シーベルト	Sv	J/kg

表4　SIと共に暫定的に維持される単位

名称	記号
オングストローム	Å
バーン	b
バール	bar
ガル	Gal
キュリー	Ci
レントゲン	R
ラド	rad
レム	rem

1 Å=0.1nm=10^{-10}m

1 b=100fm^2=10^{-28}m^2

1 bar=0.1MPa=10^{5}Pa

1 Gal=1cm/s^2=10^{-2}m/s^2

1 Ci=3.7×10^{10}Bq

1 R=2.58×10^{-4}C/kg

1 rad=1cGy=10^{-2}Gy

1 rem=1cSv=10^{-2}Sv

(注)

1．表1－5は「国際単位系」第5版，国際度量衡局1985年刊行による。ただし，1 eVおよび1 uの値はCODATAの1986年推奨値によった。

2．表4には海里，ノット，アール，ヘクタールも含まれているが日常の単位なのでここでは省略した。

3．barは，JISでは流体の圧力を表わす場合に限り表2のカテゴリーに分類されている。

4．EC閣僚理事会指令ではbar，barnおよび「血圧の単位」mmHgを表2のカテゴリーに入れている。

換算表

力	N(=10^{5}dyn)	kgf	lbf
	1	0.101972	0.224809
	9.80665	1	2.20462
	4.44822	0.453592	1

粘度　1 Pa·s(N·s/m^2)=10 P(ポアズ)(g/(cm·s))

動粘度　1m^2/s=10^{4}St(ストークス)(cm^2/s)

圧力	MPa(=10bar)	kgf/cm^2	atm	mmHg(Torr)	lbf/in^2(psi)
	1	10.1972	9.86923	7.50062×10^3	145.038
	0.0980665	1	0.967841	735.559	14.2233
	0.101325	1.03323	1	760	14.6959
	1.33322×10^{-1}	1.35951×10^{-3}	1.31579×10^{-3}	1	1.93368×10^{-2}
	6.89476×10^{-3}	7.03070×10^{-2}	6.80460×10^{-2}	51.7149	1

エネルギー・仕事・熱量	J(=10^7 erg)	kgf·m	kW·h	cal(計量法)	Btu	ft·lbf	eV
	1	0.101972	2.77778×10^{-7}	0.238889	9.47813×10^{-4}	0.737562	6.24150×10^{18}
	9.80665	1	2.72407×10^{-6}	2.34270	9.29487×10^{-3}	7.23301	6.12082×10^{19}
	3.6×10^6	3.67098×10^5	1	8.59999×10^5	3412.13	2.65522×10^6	2.24694×10^{25}
	4.18605	0.426858	1.16279×10^{-6}	1	3.96759×10^{-3}	3.08747	2.61272×10^{19}
	1055.06	107.586	2.93072×10^{-4}	252.042	1	778.172	6.58515×10^{21}
	1.35582	0.138255	3.76616×10^{-7}	0.323890	1.28506×10^{-3}	1	8.46233×10^{18}
	1.60218×10^{-19}	1.63377×10^{-20}	4.45050×10^{-26}	3.82743×10^{-20}	1.51857×10^{-22}	1.18171×10^{-19}	1

1 cal= 4.18605J（計量法）

= 4.184J（熱化学）

= 4.1855J（15℃）

= 4.1868J（国際蒸気表）

仕事率　1 PS(仏馬力)

= 75 kgf·m/s

= 735.499W

放射能	Bq	Ci
	1	2.70270×10^{-11}
	3.7×10^{10}	1

吸収線量	Gy	rad
	1	100
	0.01	1

照射線量	C/kg	R
	1	3876
	2.58×10^{-4}	1

線量当量	Sv	rem
	1	100
	0.01	1

(86年12月26日現在)

EXPERIMENTAL DATA ON POLYETHYLENE SHIELD TRANSMISSION OF QUASI-MONOENERGETIC NEUTRONS GENERATED BY 43-AND 68-MeV PROTONS VIA $^{7}Li(p,n)$ REACTION